2 - PRECISION AND CONSISTENCY OF VLBI FRAMES

Introduction

This section reports on the results of analyses and comparisons of extragalactic VLBI reference frames obtained by the IERS Analysis Centres from independent (or quasi-independent) observation programs, in order to estimate their accuracy and consistency. After a detailed study of these two sets of frames, an internal analysis of the compiled IERS celestial frame is presented. The catalogues analysed in this section are listed in table 8.

Table 8. The VLBI extragalactic reference frames compared; rotation angles (A_1, A_2, A_3) to rotate a version of a frame to the next one of the same laboratory.

Name	Label		Nb of objects	A_1	A_2	A_3	Reference
				----------(0.001")----------			
G90	RSC(GSFC)	90 R 01	72	-0.02	+0.26	-0.05	Ma and Caprette, 1990
G91	RSC(GSFC)	91 R 03	234	±0.04	±0.04	±0.03	Ma and Caprette, 1991
J90	RSC(JPL)	90 R 02	197	-0.63	-0.04	+0.32	Steppe *et al.*, 1990
				±0.06	±0.06	±0.04	Steppe *et al.*, 1991
J91	RSC(JPL)	91 R 01	241	-0.05	-0.33	-0.12	
				±0.10	±0.09	±0.07	
	RSC(JPL)	90 R 03	216				Sovers, 1991b
N90	RSC(NGS)	90 R 01	70	+0.33	-0.43	+0.01	Carter and Robertson, 1990
N91	RSC(NGS)	91 R 01	77	±0.09	±0.09	±0.08	Carter and Robertson, 1991
U90	RSC(USNO)	90 R 05	80	+0.65	+1.78	+0.39	Eubanks *et al.*, 1991a
U91	RSC(USNO)	91 R 02	80	±0.03	±0.03	±0.03	Eubanks *et al.*, 1991b
	RSC(IERS)	88 C 01	228	-0.15	-0.24	+0.21	Arias *et al.*, 1988
				±0.10	±0.10	±0.07	
	RSC(IERS)	89 C 01	209	-0.09	-0.08	+0.00	IERS, 1989
				±0.13	±0.13	±0.09	
	RSC(IERS)	90 C 01	228	+0.03	+0.06	+0.00	IERS, 1990
				±0.05	±0.04	±0.04	
	RSC(IERS)	91 C 01	396				IERS, 1991

The celestial frames studied are based on independent observations, except in two cases :
- G90 and N90 are partially based on common observations; the comparison between these two frames was not considered in the analyses,
- a small proportion of the N91 observations are also used for G91, while N91 uses none of the remaining part of G91 observations ; this slight redundancy was neglected in the comparisons.

Successive versions of the frames obtained by a given institute differ mainly in that more recent observations are accumulated in the second version - less than 10% in general ; otherwise they are based on analysis schemes that are consistent for each analysis centre. For what concerns the direction of the pole and of the origin of right ascensions, the consistency is maintained in general within a fraction of one milliarcsecond.

In order to investigate the regional deformations of the frames, or to derive statistical properties of the individual source coordinates, it is necessary first to account for the slight misalignments of

the various frames which result from the diversity of the implementation of the celestial system definitions. As there is a general tendency to match the IERS axes, the mutual misalignments between the frames studied here are smaller than 0.003".

The relative orientation between two celestial frames is obtained by computing differential rotations about the three coordinate axes on the basis of differences of coordinates of common objects. A source common to the two frames and in the direction of unit vector $\vec{D}$ has two sets of coordinates, one in frame 1 and one in frame 2. Provided that there exists no relative deformations between the frames, and that they only differ by a rotation, the transformation between the two celestial reference frames can be written as:

$$\vec{D}_2 = M \vec{D}_1 \qquad (1)$$

where the rotation matrix M is

$$M = \begin{bmatrix} 1 & A_3 & -A_2 \\ -A_3 & 1 & A_1 \\ A_2 & -A_1 & 1 \end{bmatrix}$$

A_1, A_2, A_3 are the infinitesimal rotation angles about x,y and z axes respectively, which express the rotation of frame 2 to frame 1. In each frame, the x-axis is in the direction of the origin of right ascensions, the z-axis points to the celestial pole and the y-axis completes a direct triad.

The differences between the equatorial coordinates of a source common to two frames are, to the first order with respect to A_1, A_2, and A_3:

$$\alpha_1 - \alpha_2 = A_1 \cos\alpha_2 \sin\delta_2 / \cos\delta_1 + A_2 \sin\alpha_2 \sin\delta_2 / \cos\delta_1 - A_3 \cos\delta_2 / \cos\delta_1 \qquad (2)$$

$$\delta_1 - \delta_2 = -A_1 \sin\alpha_2 + A_2 \cos\alpha_2 \qquad (3)$$

The three unknowns A_1, A_2 A_3 are estimated by a least squares fit for a selection of sources common to the two frames. The equations are weighted according to the uncertainties of the coordinates, with a lower limit of 0.00025" on each individual value. Earlier studies have shown that the use of added variance or scaling factors of the formal uncertainties is not necessary.

Analysis of four 1990 VLBI extragalactic reference frames

This section gives the results of statistical analyses of four VLBI frames which were available for the compilation of RSC(IERS) 90 C 01, published in the IERS Annual Report for 1989. The analyses are based on the differences of coordinates in the five pairs of independent catalogues, after taking out relative rotation angles. The latter, listed in table 9, are estimated by restricting the set of common sources considered to those which had been retained as primary in the compilation of RSC(IERS) 90 C 01, *i.e.*, whose coordinates were the most consistent in the various frames (see p.46).

Table 9. Relative orientations of the four 1990 individual frames. N is the number of common sources considered, σ is the rms post-fit residual. Units for A_1, A_2, A_3 and σ: 0.001".

Frame 1-Frame 2	N	A_1	A_2	A_3	σ
U90 - G90	30	-0.33	+0.28	-0.33	0.49
		±0.11	±0.10	±0.09	
G90 - J90	28	-1.86	-2.97	+0.36	0.35
		±0.09	±0.08	±0.06	
N90 - J90	27	-1.87	-1.30	+0.27	0.43
		±0.12	±0.11	±0.08	
N90 - U90	27	+0.28	+0.31	+0.36	0.53
		±0.12	±0.12	±0.11	
U90 - J90	36	-1.91	-2.61	+0.06	0.48
		±0.11	±0.10	±0.07	

Number of observations and formal uncertainties

Figure 6 shows the relationship between the formal uncertainty of the source coordinates and the number of observed delays for the three catalogues for which this information was available(G90, J90, U90). The formal uncertainty follows a law in $N^{-0.5}$ (slope = -1 on the graph) for a $50 < N < 3000$. For larger N it meets a floor at 0.06 mas in $\alpha.\cos\delta$ and 0.13 mas in declination, in the case of GSFC.

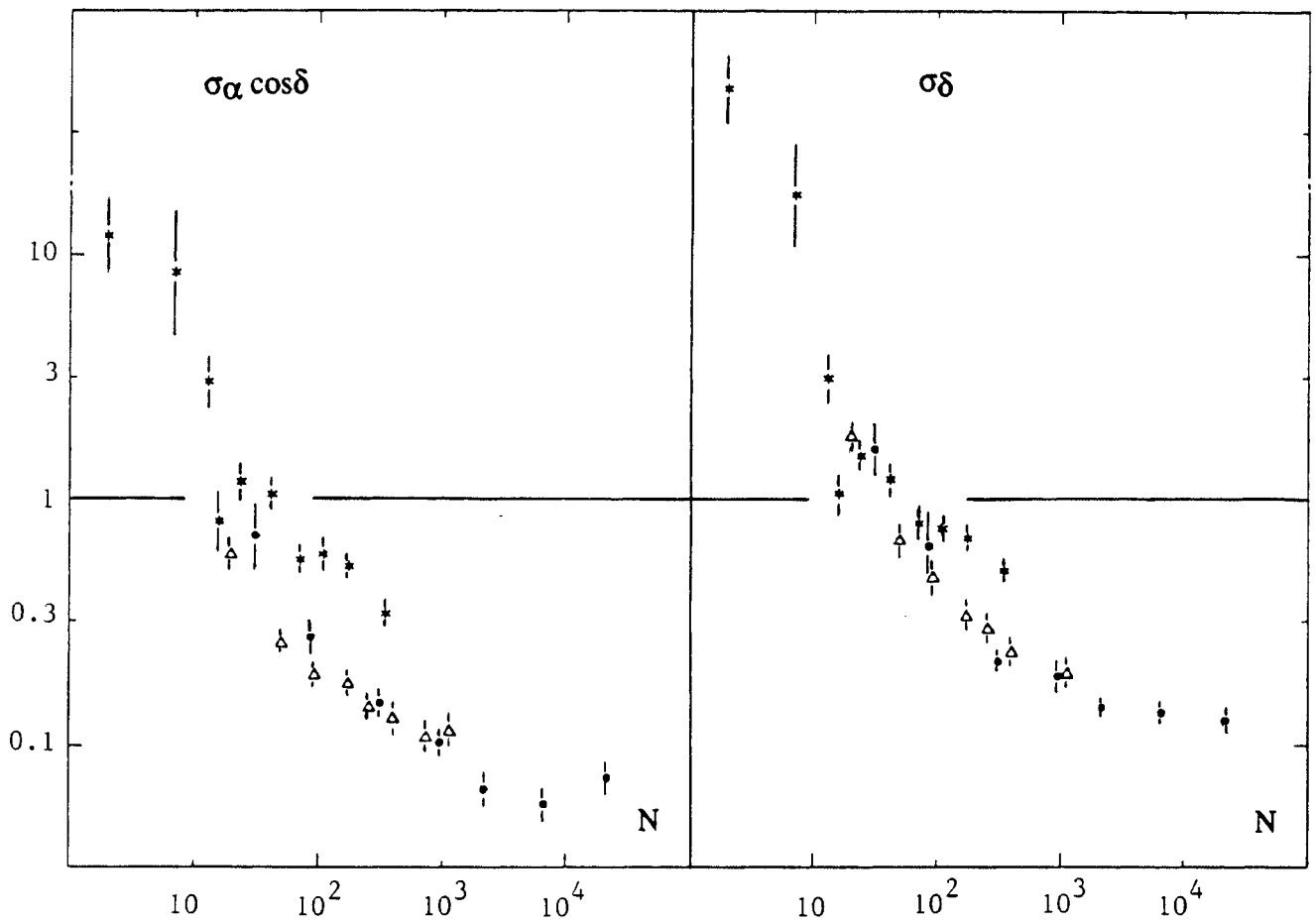

Figure 6. Formal uncertainties of source coordinates as a function of the number of observations.
Unit: 0.001"
- • GSFC (G90, 72 sources)
- * JPL (J90, 197 sources)
- Δ USNO (U90, 80 sources)

Consistency of the coordinates of 39 objects common to the four catalogues

In this section, we consider the residual differences in right ascension and in declination of the 39 sources which are common to the four catalogues, obtained by removing the two-by-two rotation angles of table 9. The mean differences of the source coordinates in a given catalogue with respect to the other three (or two) are listed in table 10. The estimated uncertainty of the mean differences per source ranges from 0.2 to 0.5 mas in general. The data are summarized in table 11.

Table 10. Mean coordinate residual differences, one catalogue - the others

Source	R.A. *cosδ 0.001"				Declination 0.001"			
	GSFC	JPL	NGS	USNO	GSFC	JPL	NGS	USNO
0048-097	0.16	-0.49	0.18	0.26	0.32	-1.32	0.52	0.76
	0.13	0.77	0.15	0.16	0.19	1.32	0.30	0.42
	0.57	0.78	0.58	0.49	1.00	1.36	1.02	0.89
0106+013	-0.03	0.06	-0.08	0.01	-0.67	-0.67	-0.36	1.35
	0.03	0.40	0.03	0.16	0.14	0.53	0.20	0.25
	0.31	0.41	0.31	0.28	0.44	0.57	0.46	0.42
0119+041	-0.23	0.35	-0.12	-0.11	2.95	-4.22	0.65	1.82
	0.18	0.75	0.10	0.07	0.35	1.28	0.30	0.12
	0.56	0.76	0.54	0.45	0.97	1.31	0.96	0.79
0212+735	-0.05	-0.01	-0.31	0.26	0.03	0.01	0.19	-0.16
	0.11	0.45	0.22	0.20	0.12	0.37	0.20	0.20
	0.37	0.49	0.41	0.36	0.32	0.41	0.36	0.32
0229+131	0.03	-0.32	0.09	0.23	-0.45	0.46	-0.69	0.30
	0.04	0.41	0.07	0.28	0.13	0.95	0.20	0.43
	0.35	0.44	0.36	0.37	0.75	0.99	0.76	0.71
0234+285	0.23	0.19	0.18	-0.46	-0.20	-0.16	-0.26	0.47
	0.07	0.35	0.13	0.09	0.12	0.38	0.20	0.12
	0.26	0.36	0.29	0.24	0.31	0.41	0.35	0.28
0235+164	0.15	-0.18	0.59	-0.31	-0.64	0.85	-1.51	0.58
	0.11	0.42	0.14	0.09	0.34	0.38	0.40	0.11
	0.32	0.44	0.33	0.28	0.44	0.49	0.49	0.39
0300+470	0.29	0.19	0.10	-0.45	-0.20	-0.15	-0.05	0.32
	0.09	0.40	0.18	0.09	0.13	0.39	0.20	0.12
	0.30	0.42	0.34	0.27	0.32	0.42	0.35	0.29
0420-014	-0.37	0.23	-0.40	0.28	-1.25	0.98	-1.83	1.08
	0.03	0.33	0.03	0.09	0.14	0.43	0.20	0.11
	0.24	0.33	0.24	0.21	0.34	0.46	0.37	0.31
0528+134	-0.02	0.42	0.16	-0.51	-0.91	0.48	-1.49	1.12
	0.04	0.35	0.07	0.09	0.13	0.42	0.20	0.10
	0.26	0.36	0.26	0.23	0.33	0.45	0.36	0.30
0552+398	0.08	0.19	0.07	-0.29	-0.09	-0.29	-0.10	0.41
	0.08	0.23	0.15	0.09	0.12	0.34	0.20	0.13
	0.19	0.26	0.23	0.19	0.28	0.37	0.33	0.27
0727-115	-0.95	0.80	-0.20	-0.03	-1.34	1.07	-1.76	1.00
	0.06	0.41	0.06	0.10	0.15	0.52	0.20	0.21
	0.30	0.42	0.30	0.26	0.42	0.55	0.44	0.39

Line 1: Average difference with the other three (two) catalogues
Line 2: Formal uncertainty in the catalogue
Line 3: Formal uncertainty of the difference (derived from the quadratic combination of the formal uncertainties of the catalogues considered in the differences)

Table 10. (cont.) Mean coordinate residual differences, one catalogue - the others

Source	R.A. *cosδ 0.001"				Declination 0.001"			
	GSFC	JPL	NGS	USNO	GSFC	JPL	NGS	USNO
0742+103	0.05	-0.08	0.73	-0.44	-1.09	0.73	-1.63	1.07
	0.06	0.30	0.10	0.10	0.19	0.39	0.40	0.10
	0.23	0.31	0.24	0.21	0.34	0.47	0.49	0.36
0851+202	-0.27	0.20	0.06	-0.06	-0.04	-0.53	-0.37	0.80
	0.04	0.28	0.07	0.11	0.12	0.37	0.20	0.09
	0.22	0.29	0.22	0.20	0.29	0.40	0.34	0.27
0923+392	-0.04	-0.16	-0.08	0.23	-0.22	0.03	-0.25	0.28
	0.08	0.23	0.12	0.14	0.12	0.26	0.20	0.09
	0.21	0.26	0.23	0.21	0.23	0.30	0.28	0.22
1034-293	-0.77	1.54	0.34	-1.25	-0.04	1.55	0.47	-1.83
	0.18	0.89	0.16	0.20	0.24	0.78	0.30	0.62
	0.67	0.91	0.66	0.57	0.74	0.89	0.77	0.80
1055+018	-0.28	1.00	0.38	-1.06	-1.27	0.08	-1.30	1.63
	0.03	0.30	0.04	0.15	0.15	0.44	0.30	0.27
	0.24	0.31	0.24	0.23	0.39	0.51	0.47	0.42
1253-055	-0.97	2.02	-0.14	-1.28	0.05	1.08	-0.40	-0.85
	0.09	0.42	0.15	0.12	0.22	0.72	0.40	0.27
	0.32	0.44	0.34	0.29	0.59	0.78	0.68	0.56
1308+326	0.12	0.06	-0.02	-0.12	-0.27	0.04	-0.26	0.32
	0.06	0.24	0.10	0.14	0.13	0.49	0.20	0.16
	0.21	0.26	0.22	0.21	0.39	0.52	0.42	0.35
1334-127	-0.50	1.16	0.04	-0.86	-0.84	0.49	-0.38	0.32
	0.10	0.47	0.10	0.16	0.20	0.77	0.30	0.42
	0.37	0.49	0.37	0.33	0.65	0.83	0.69	0.65
1404+286	0.29	-0.14	0.37	-0.30	0.39	-0.79	0.58	0.14
	0.05	0.29	0.09	0.16	0.13	0.67	0.20	0.20
	0.24	0.31	0.25	0.24	0.51	0.69	0.53	0.46
1418+546	-0.03	0.12	-0.60	0.29	-0.25	0.35	-0.67	0.26
	0.16	0.36	0.23	0.15	0.18	0.56	0.30	0.16
	0.32	0.40	0.36	0.30	0.45	0.60	0.51	0.41
1502+106	0.02	0.10	0.55	-0.48	-0.62	-0.05	0.17	0.35
	0.04	0.28	0.06	0.16	0.15	0.70	0.20	0.27
	0.23	0.30	0.24	0.23	0.55	0.73	0.57	0.51
1548+056	0.09	-0.34	0.41	0.01	-0.89	-0.38	-0.14	1.07
	0.04	0.37	0.04	0.12	0.14	0.81	0.20	0.29
	0.28	0.38	0.28	0.25	0.62	0.84	0.64	0.57
1611+343	0.06	0.02	-0.16	0.04	-0.14	0.27	-0.40	0.09
	0.15	0.31	0.12	0.11	0.20	0.76	0.20	0.21
	0.28	0.34	0.26	0.24	0.59	0.79	0.59	0.51
1633+382	-0.31	0.53	-0.39	-0.06	-0.40	0.56	-0.45	0.01
	0.07	0.29	0.13	0.13	0.12	0.69	0.20	0.21
	0.24	0.31	0.26	0.23	0.52	0.71	0.55	0.47
1730-130	-0.33	0.90	-0.60	-0.28	0.48	-1.72	1.73	0.25
	0.07	0.45	0.10	0.16	0.16	0.96	0.20	0.48
	0.34	0.46	0.35	0.31	0.78	1.01	0.78	0.75
1741-038	0.10	0.08	0.22	-0.29	-0.49	-0.41	0.69	0.28
	0.03	0.39	0.04	0.10	0.15	0.88	0.20	0.31
	0.29	0.40	0.29	0.25	0.68	0.91	0.69	0.61
1749+096	0.05	-0.23	0.23	0.04	-0.28	-0.69	0.69	0.42
	0.04	0.35	0.06	0.12	0.14	0.93	0.20	0.30
	0.26	0.36	0.27	0.24	0.71	0.96	0.72	0.63
1803+784	-0.05	0.03	-0.29	0.19	-0.10	0.19	-0.27	0.06
	0.11	0.88	0.22	0.10	0.12	0.73	0.20	0.17
	0.64	0.89	0.66	0.54	0.54	0.75	0.57	0.47

Table 10. (cont.) Mean coordinate residual differences, one catalogue - the others

Source	R.A. *cosδ 0.001"				Declination 0.001"			
	GSFC	JPL	NGS	USNO	GSFC	JPL	NGS	USNO
1921-293	0.81	0.11	-0.44	-0.35	-2.04	1.89	-0.63	-0.11
	0.09	0.73	0.14	0.14	0.20	1.08	0.30	0.44
	0.53	0.74	0.54	0.45	0.85	1.13	0.88	0.79
1923+210	0.34	0.14	-1.70	0.76	0.62	0.44	-1.54	0.18
	0.39	0.38	0.41	0.22	1.09	0.72	1.10	0.30
	0.50	0.52	0.51	0.45	1.22	1.16	1.23	1.03
2121+053	-0.25	0.15	-0.03	0.03	-0.88	0.30	0.05	0.26
	0.04	0.39	0.04	0.13	0.13	0.71	0.20	0.24
	0.29	0.40	0.29	0.26	0.55	0.74	0.57	0.49
2128-123	0.39	0.75	-0.25	-0.84	-2.06	-0.86	-1.12	2.98
	0.32	0.45	0.41	0.28	0.32	0.85	0.40	0.87
	0.49	0.56	0.56	0.49	0.92	1.03	0.95	1.04
2145+067	-0.31	0.18	-0.17	0.14	-1.09	0.55	-0.36	0.41
	0.04	0.39	0.04	0.10	0.13	0.68	0.20	0.21
	0.29	0.40	0.29	0.25	0.52	0.70	0.54	0.47
2200+420	-0.26	-0.28	-0.22	0.60	-0.23	-0.17	-0.29	0.52
	0.09	0.47	0.13	0.10	0.12	0.49	0.20	0.13
	0.35	0.48	0.36	0.30	0.38	0.51	0.41	0.34
2216-038	0.15	-0.07	0.02	-0.04	-1.83	1.59	-0.79	0.15
	0.04	0.45	0.04	0.10	0.15	0.84	0.30	0.24
	0.33	0.45	0.33	0.28	0.64	0.87	0.69	0.57
2234+282	-0.30	-0.34	0.00	0.54	-0.31	-0.28	-0.06	0.54
	0.08	0.44	0.11	0.09	0.13	0.49	0.20	0.13
	0.33	0.45	0.34	0.28	0.38	0.51	0.41	0.34
2345-167	0.63	-0.71	-0.11	0.36	-1.14	1.28	0.09	-0.58
	0.14	0.69	0.17	0.16	0.18	0.96	0.30	0.42
	0.52	0.71	0.53	0.45	0.76	1.01	0.80	0.72

Table 11. Statistics of the average differences of coordinates in one catalogue with the other three (two). Unit: 0.001"

RSC	Right ascension*cosδ				Declination			
	1	2	3	4	1	2	3	4
G90	-0.06	0.37	0.36	1.05	-0.45	0.95	0.60	1.65
J90	0.21	0.58	0.48	1.25	0.07	1.04	0.77	1.15
N90	-0.04	0.41	0.37	1.16	-0.35	0.84	0.63	1.67
U90	-0.14	0.49	0.32	1.61	0.46	0.89	0.56	1.76

1: arithmetic mean of the differences
2: rms difference
3: rms formal uncertainty of the differences
4: rms ratio of difference/formal uncertainty

Figure 7 is similar to figure 6, the plotted values being the residual position differences of table 10 (line 1). The residual position differences in right ascension follow roughly a law in $N^{-0.5}$, while in the case of the declinations the accumulation of observations does not diminish the dispersion in the same proportion.

Figures 8a and 8b give the plots of the formal uncertainty and of the residual position differences as a function of right ascension and of declination. The most striking feature is the clear degradation of the residual position differences in declination for decreasing declinations, which is not echoed in full size by a similar trend in the formal uncertainties.

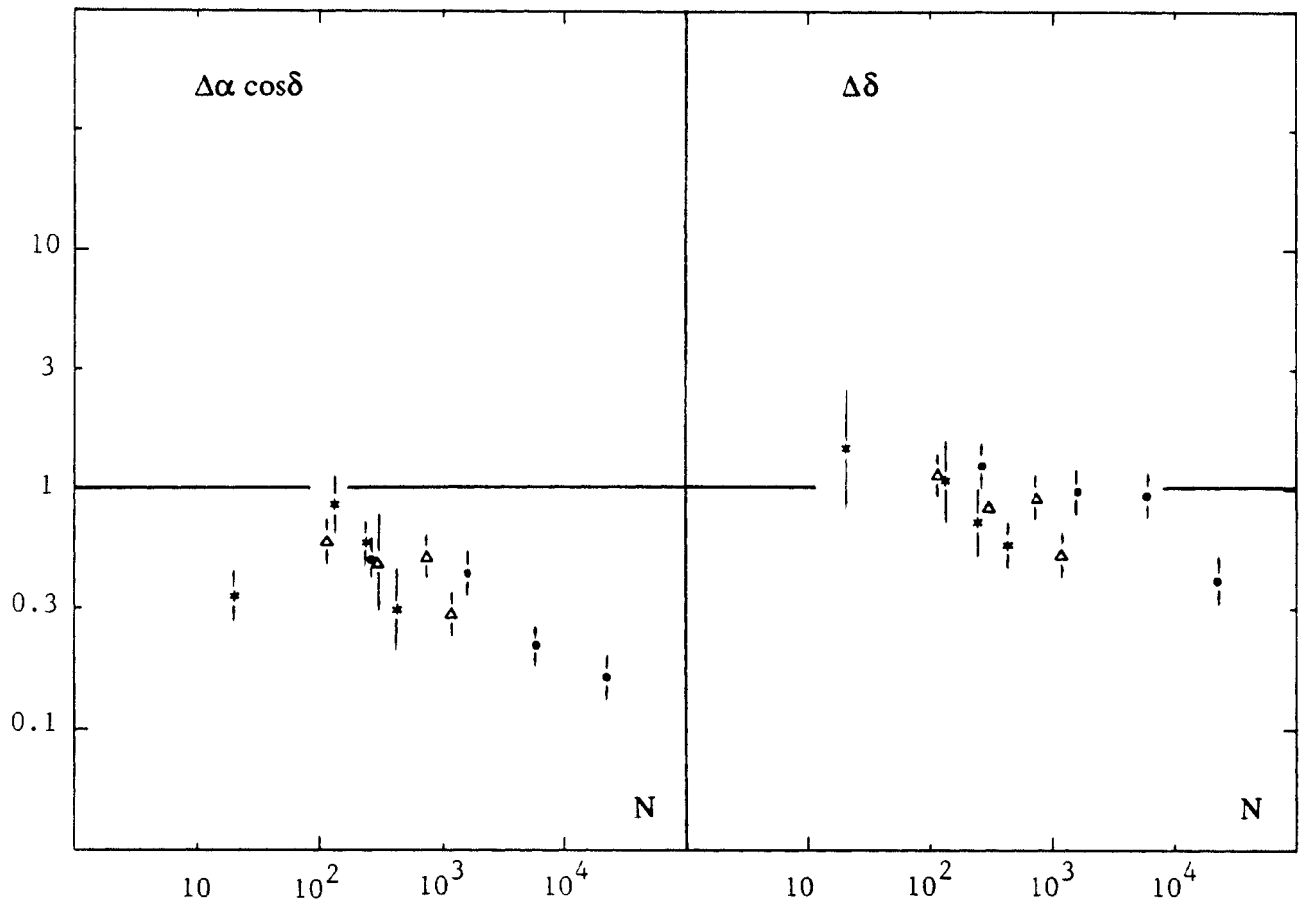

Figure 7. 39 sources common to the four catalogues: mean residual position differences of the coordinates in one catalogue with respect to the other ones, after taking out the relative rotations, as a function of the number of observations. Unit: 0.001"

- • GSFC (G90)
- * JPL (J90)
- Δ USNO (U90)

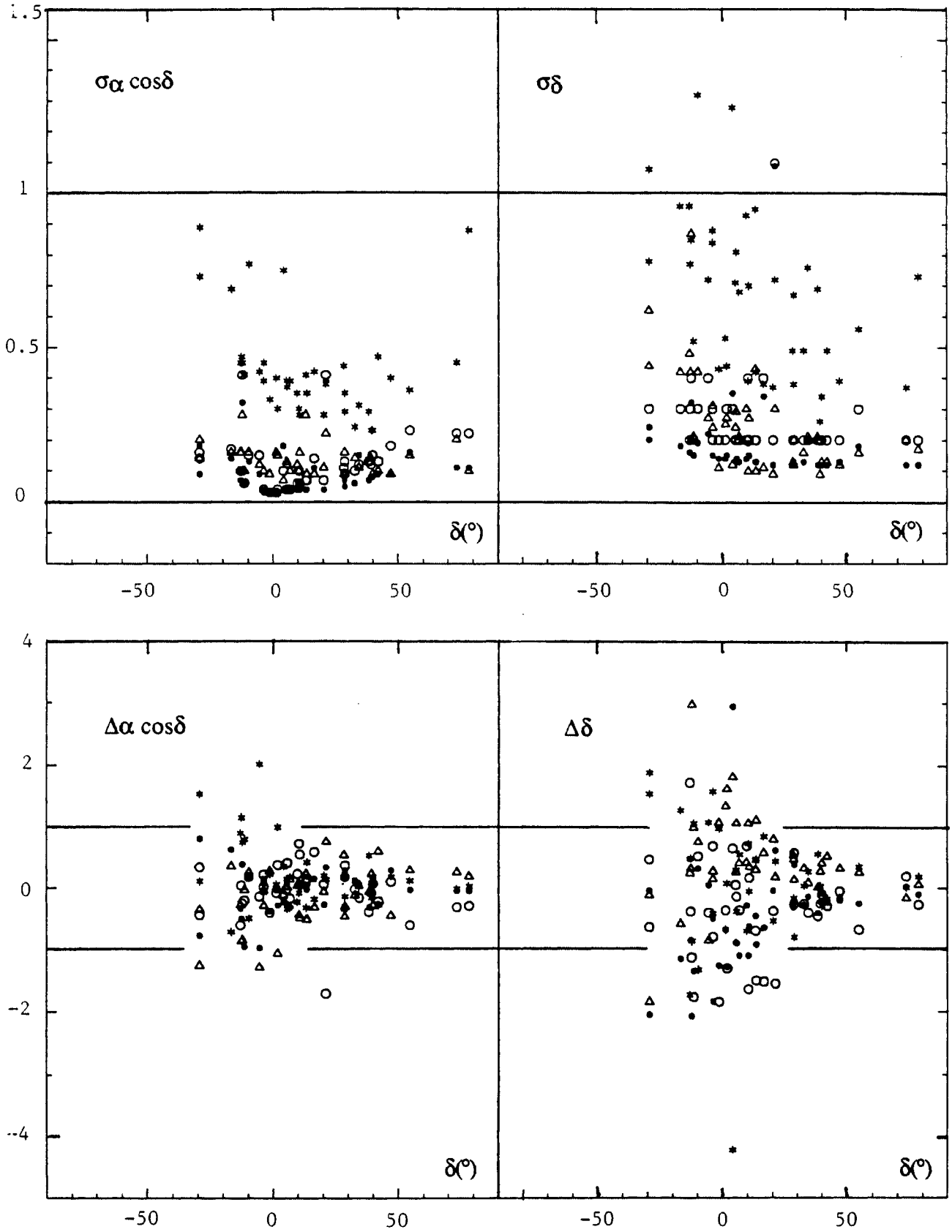

Figure 8a. 39 sources common to four catalogues : formal uncertainties (upper part) and residual position differences (lower part) as a function of declination . Unit: 0.001"
Catalogues G90 (•), J90 (*), N90 (o), U90 (Δ).

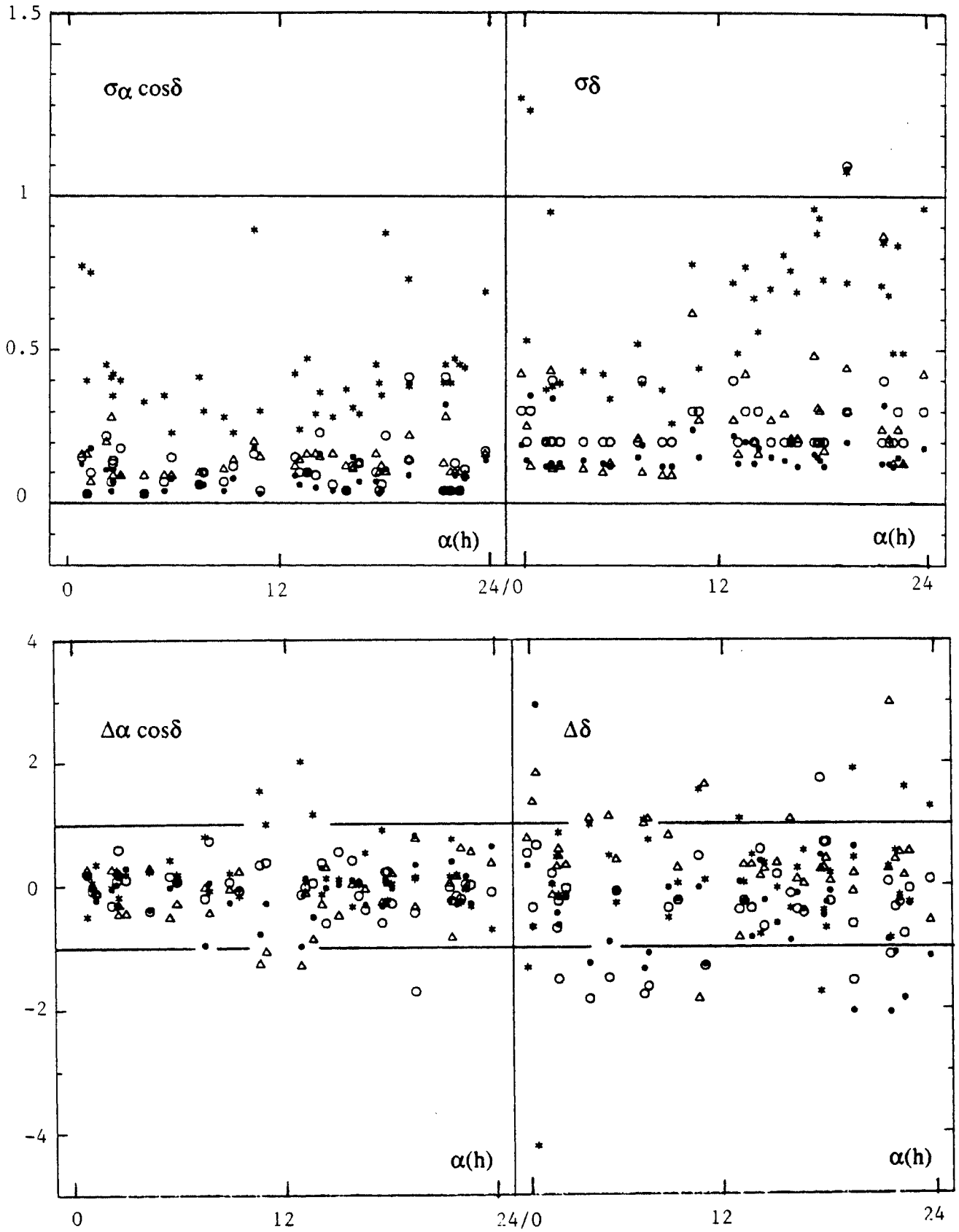

Figure 8b. 39 sources common to four catalogues : formal uncertainties (upper part) and residual position differences (lower part) as a function of right ascension. Unit: 0.001".
Catalogues G90 (•), J90 (*), N90 (o), U90 (Δ).

Using the five sets of residual position differences between pairs of independent catalogues after taking out the relative rotations, we consider two classes of sources, according to their declinations. From figures 8a and 8b, we split the sets of sources at declination 0° for the right ascension residual position differences and declination +20° for the declination residual position differences. Having thus defined four classes with homogeneous behaviours, we perform the three corner hat method : for a given class, the observed variance of the residual position differences in a pair of catalogues is equal to the sum of the intrisic true variances of the positions in each of the two catalogues. By forming all possible triangles between independent catalogues, the true precision of the source coordinates is estimated (see table 12). In the best case, the true uncertainty of the coordinates is about 0.2 mas ; in the worst case, the true uncertainty is still under 1 mas.

Table 12. Estimated position uncertainty of sources observed in four programs.
Unit : 0.001"

	Class:	$\delta \geq 0$	$\delta \geq 20°$	$\delta < 0$	$\delta < 20°$
Cat.	Coordinate:	$\alpha \cos\delta$	δ	$\alpha \cos\delta$	δ
	Nb sources:	27	15	12	24
G90		0.20	0.23	0.34	0.81
J90		0.24	0.23	0.67	0.85
N90		0.27	0.28	0.18	0.85
U90		0.33	0.31	0.42	0.67

Possible systematic effects related to physical characteristics in the 39 objects common to G90, J90, N90, U90.

The influence of various physical characters of the source, as given by Preston *et al.* (1985), is investigated.

Figures 9-12 show the average position differences behaviour as a function of

- the type of object,
- the total flux,
- the redshift,
- the spectral index defined by Preston *et al.* (1985, p.1599).

In order to disantangle the low declination effect, the plots of raw residual differences are complemented with plots where they are corrected by a simple empirical function of declination. As there is no particular correlation of low declinations with any of the physical characteristics considered here, we conclude from the second series of plots that there is no obvious influence of the physical characteristics of the objects on the dispersion of the source coordinates.

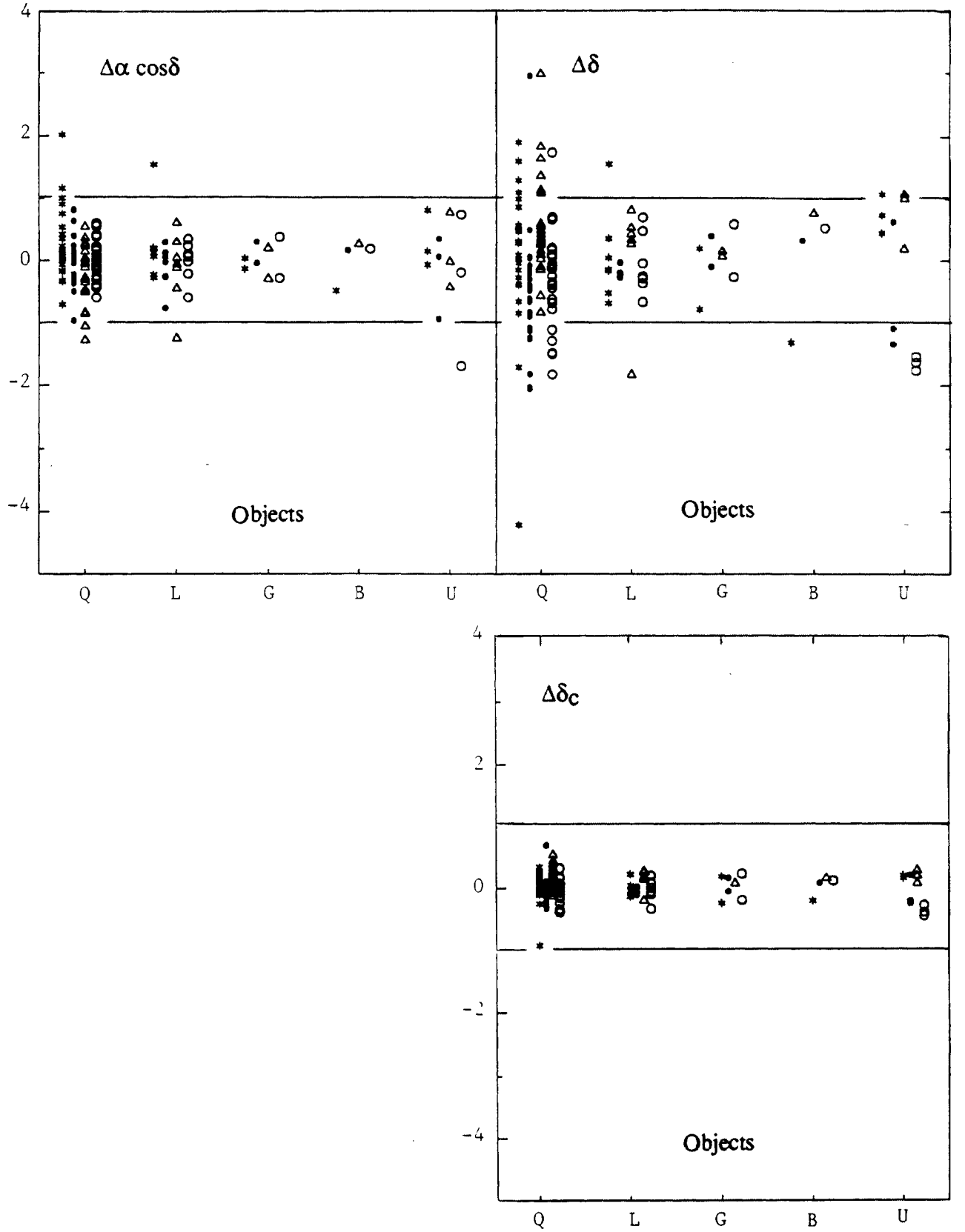

Figure 9. Coordinate residual position differences as a function of the type of object.
Q : quasar ; BL : B Lac object ; G : galaxy ; B : Blue object ; U : unknown.
Upper part : raw residual position differences ; lower part : residual declination differences corrected for an effect in declination. Unit: 0.001".
Catalogues G90 (•), J90 (*), N90 (o), U90 (Δ).

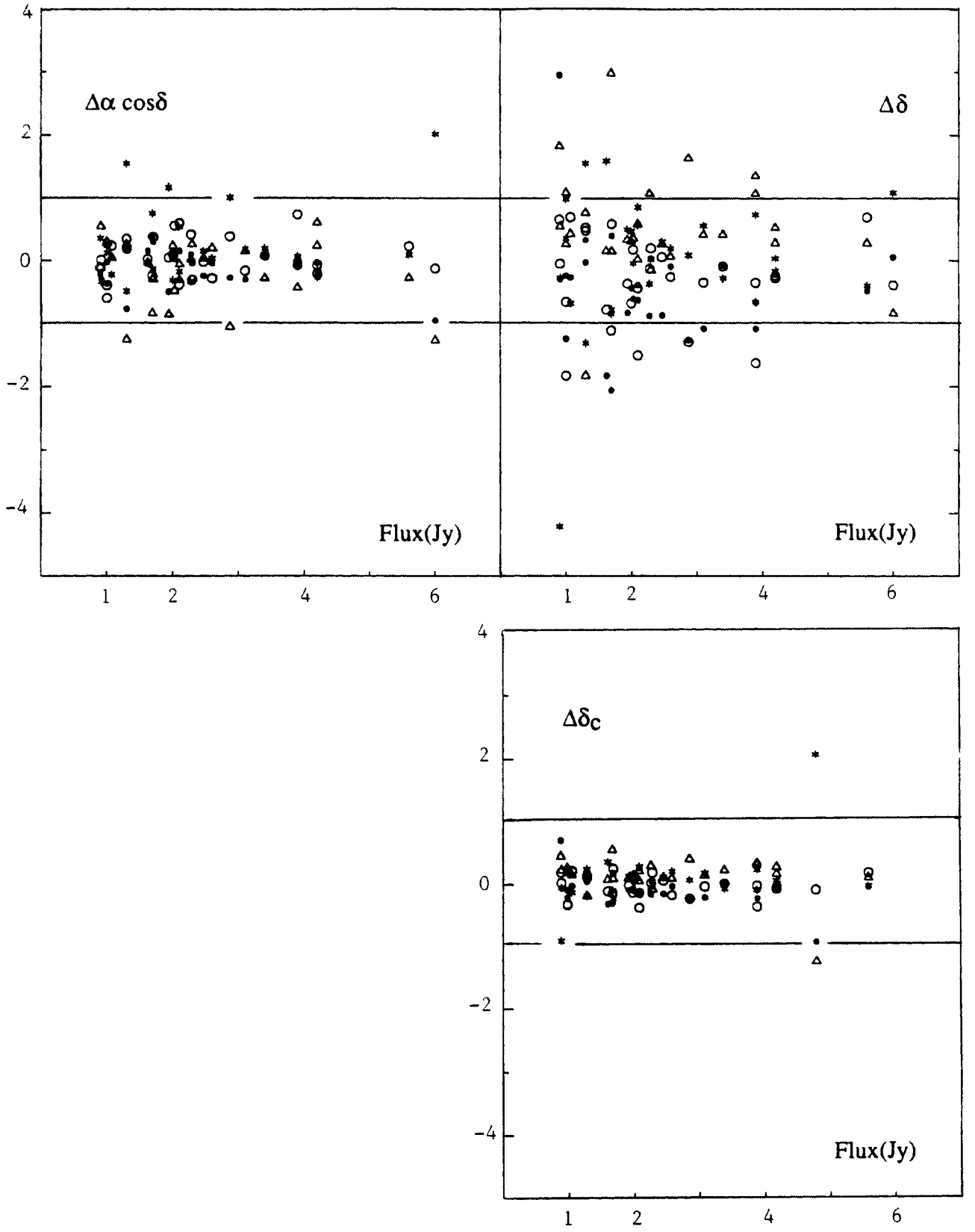

Figure 10. Coordinate residual position differences as a function of total flux.
Upper part : raw residual position differences ; lower part : residual declination differences corrected for an effect in declination. Unit: 0.001".
Catalogues G90 (•), J90 (*), N90 (o), U90 (Δ).

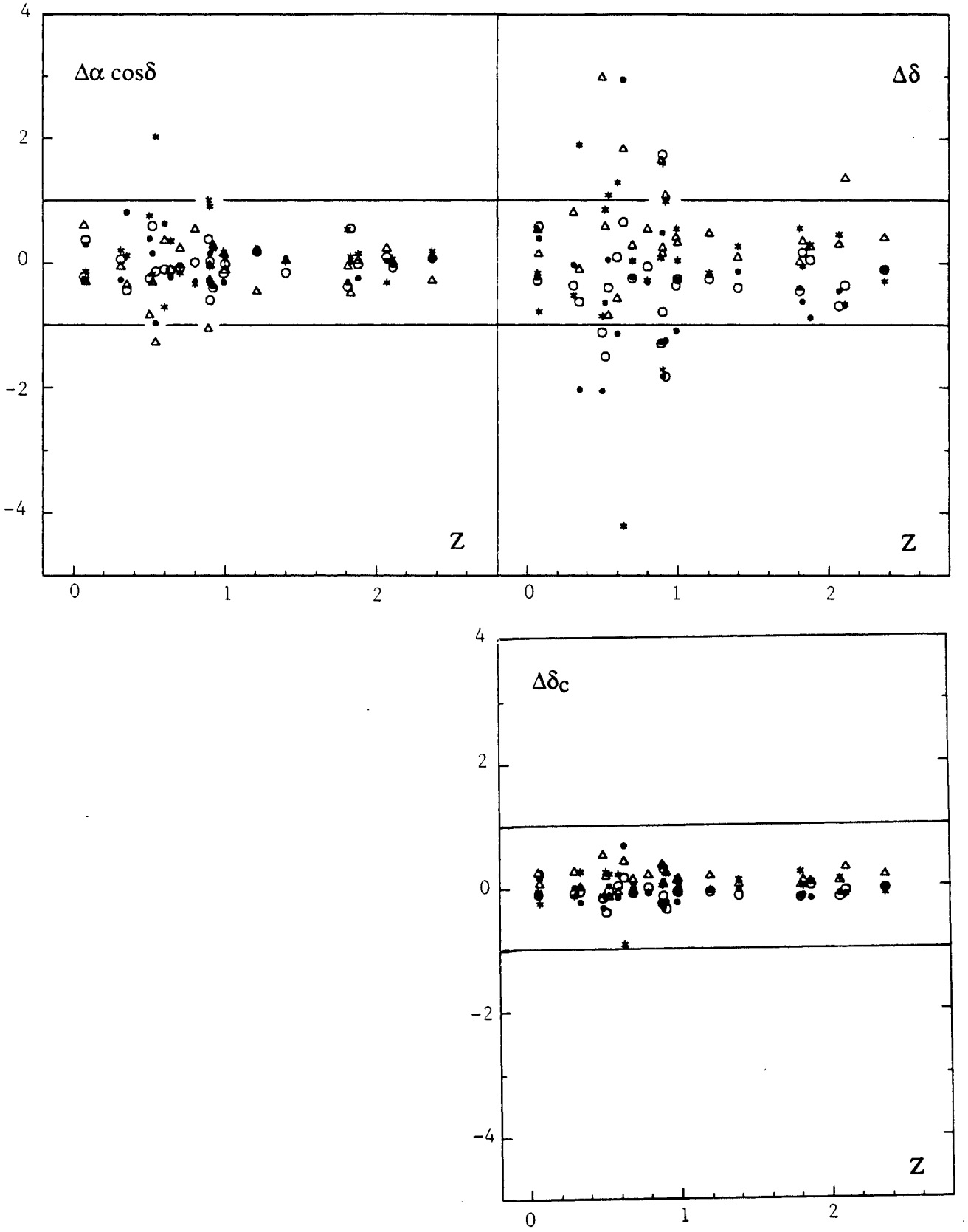

Figure 11. Coordinate residual position differences as a function of redshift
Upper part : raw residual position differences ; lower part : residual declination differences corrected for an effect in declination. Unit: 0.001".
Catalogues G90 (•), J90 (*), N90 (o), U90 (Δ).

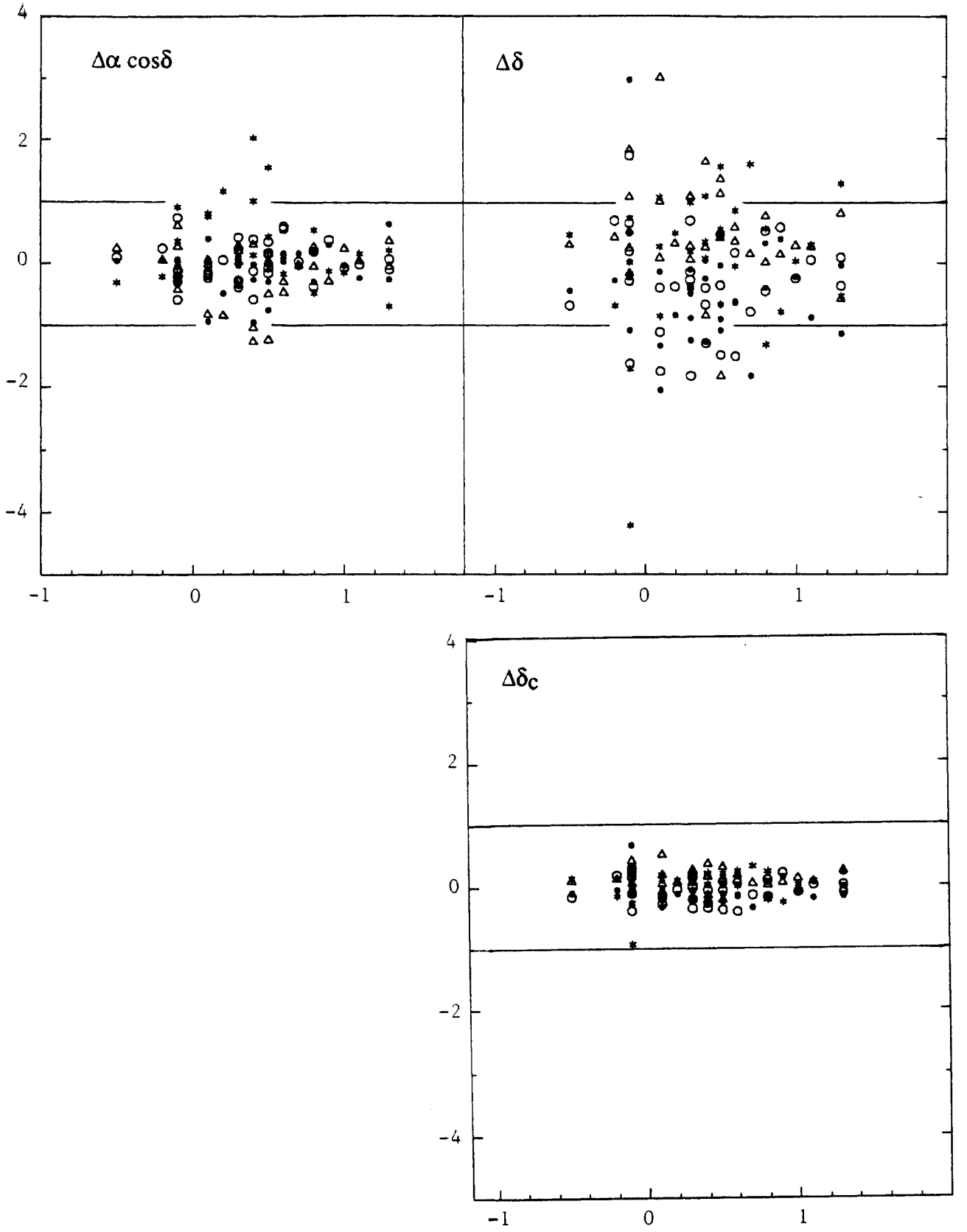

Figure 12. Coordinate residual position differences as a function of spectral type.
Upper part : raw residual position differences ; lower part : residual declination differences corrected for an effect in declination. Unit: 0.001".
Catalogues G90 (•), J90 (*), N90 (o), U90 (Δ).

Comparison of four 1991 VLBI extragalactic reference frames

Analyses of four VLBI extragalactic reference frames submitted to IERS in 1991 are presented here. They have been obtained in the 1991 global solutions at the Goddard Space Flight Center (GSFC), at the Jet Propulsion Laboratory (JPL), at the US National Geodetic Survey (NGS) and at the US Naval Observatory (USNO).

In order to assess the astrometric quality of the four individual frames we have performed comparisons two by two to evaluate the relative orientations between axes and to determine the existence of relative regional deformations.

Table 13 presents the four individual VLBI frames compared. In all cases the pole of the celestial reference frame is fixed by the standard J 2000.0 precession and the IAU 1980 Theory of nutation. In the four solutions, corrections to the position of the celestial pole given by the models are adjusted simultaneously with the astrometric and geodetic parameters. In this process, each series of the celestial pole offsets, $d\psi$ and $d\varepsilon$, is referred to an arbitrary value at some epoch, which gives rise to small offsets in the effective poles of the various frames.

Table 13. Individual VLBI axtragalactic reference frames compared in the analyses.

Frame			Number of objects	Declination interval	Observational data
G91	RSC(GSFC)	91 R 03	234	-81°, +85°	CDP
J91	RSC(JPL)	91 R 01	241	-45°, +85°	DSN
N91	RSC(NGS)	91 R 01	77	-81°, +79°	POLARIS/IRIS (CDP)
U91	RSC(USNO)	91 R 02	80	-41°, +79°	NAVNET

The origin of right ascensions is fixed a priori in the VLBI solutions. In RSC(GSFC) 91 R 03 the conventional right ascension of 3C273B is used to define the origin on the equator. In RSC(NGS) 91 R 01, the radio source coordinates are adjusted by fixing the mean of the right ascensions of nine radio sources to values which were obtained in previous adjustments referred to conventional right ascension of 3C273B. JPL and USNO frames are aligned as closely as possible to the IERS Celestial Reference Frame. In RSC(JPL) 91 R 01 the right ascension and declination of 0851+202 and the declination of 0234+285, both of which are primary sources in the IERS frame, are held fixed at their values in RSC(IERS) 89 C 01. The NAVNET reference frame is obtained in a two step process; in the first step the right ascension of the source 2216-038 is fixed at the value given in RSC RSC(IERS) 90 C 01; the right ascension and declination of 0202+149 and the declination of 0742+103 are fixed in a second step to the values obtained in the first one. In all frames, the standard errors are the values obtained from the adjustment, and they can be interpreted as the limit that would be attained in the absence of unmodeled systematic errors.

The relative rotation angles in the four pairs of frames, estimated by a weighted least squares fit over all common sources, are in table 14. In most cases the directions of axes between the 1991 individual realisations of the VLBI celestial reference frame are consistent better than 0.0015" for A_1 and A_2, with uncertainties at the level of 0.0001"; when the effect of inhomogeneous fixing of the levels of $d\psi$, $d\varepsilon$ is taken into account, the largest difference is 0.0004". The origins of right ascensions, arbitrarily fixed in each frame, differ by less than 0.0003", as indicated by the values of the angle A_3.

Table 14. Relative orientations of the four 1990 individual frames. N indicates the number of common sources considered, σ indicates the rms of the post-fit residuals. Units for A_1, A_2, A_3 and σ: 0.001".

Frame 1-Frame 2	N	A_1	A_2	A_3	σ
N91 - G91	73	+0.196 ±0.038	+0.911 ±0.036	+0.003 ±0.033	0.27
U91 - G91	37	+0.461 ±0.095	+1.740 ±0.094	+0.053 ±0.077	0.63
G91 - J91	150	-1.406 ±0.088	-2.823 ±0.084	+0.219 ±0.065	0.35
N91 - J91	62	-1.131 ±0.119	-1.881 ±0.112	+0.232 ±0.088	0.43
N91 - U91	48	-0.289 ±0.101	-0.815 ±0.096	+0.006 ±0.084	0.53
U91 - J91	74	-0.637 ±0.108	-1.065 ±0.099	+0.198 ±0.079	0.48

Relative deformations

The different network geometries might cause regional deformations in the VLBI frames produced by the individual groups. Source positions in the northern hemisphere are somewhat better determined than in the southern hemisphere. The precision of declinations near the equator strongly depends on the length of the North-South baseline components and on the strategies of observation. A lack of sensitivity to this declination range is noticeable with some networks which are predominantly oriented in the East-West direction.

We have investigated the existence of regional deformations between pairs of frames by comparing the positions of common radio sources after removing the relative orientations previously evaluated (table 14). The position differences of the sources common to the pairs of catalogues are shown in figures 13a through 13f. Most of the position differences are smaller than 0.002". However, systematic effects are present in some pairs of frames. Only a few systematic differences larger than 0.0005" between frames elaborated at NGS and GSFC (figure 13a) are observed. The distribution of vectors in figure 13b suggests that there exists a deformation between NGS and JPL frames with a general effect in declination and a smaller effect in right ascension in the interval 20h - 4h. In the comparison between NGS and USNO frames (figure 13c) most vectors are oriented in the North-South direction, representing a systematic effect in declination only. The vectors representing the positions differences of sources common to USNO and GSFC in figure 13d are oriented in the South-North direction, showing a deformation in declination. Vectors seem to follow a random distribution in the comparison USNO - JPL of figure 13e. In figure 13f, the systematic differences at low declinations already noticed in NGS-JPL (figure 13b) are confirmed for the additional sources common to GSFC and JPL.

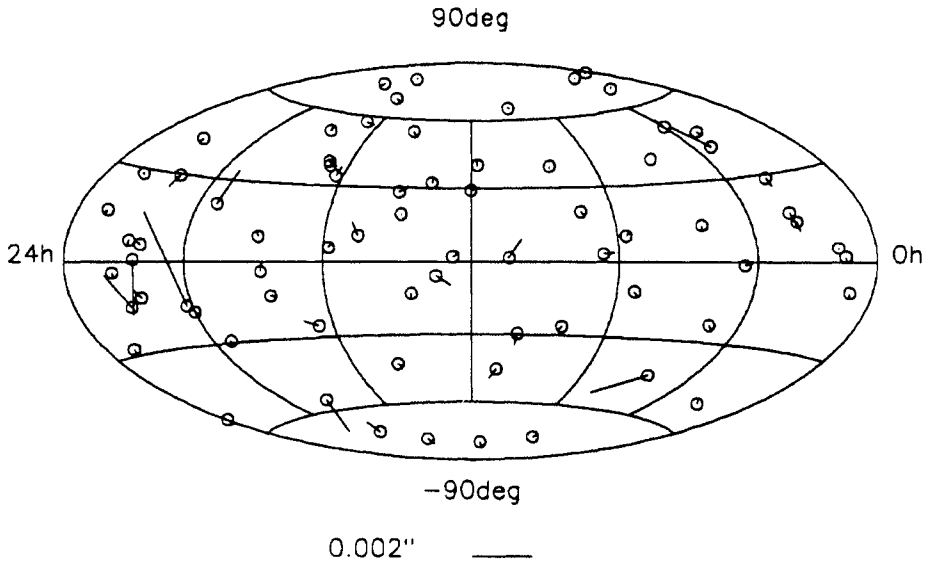

Figure 13a. Position differences of radio sources common to NGS and GSFC frames in Aitoff projection. The solid lines join the NGS positions (circles) to the GSFC positions after removing the global rotations between the two frames. The scale of the vector module is shown in the figure.

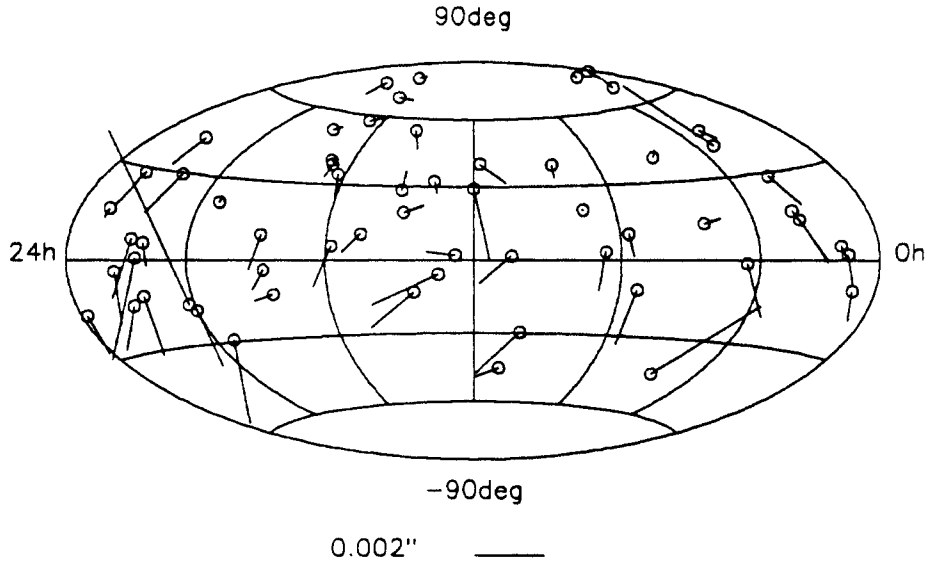

Figure 13b. Position differences of radio sources common to NGS and JPL frames in Aitoff projection. The solid lines join the NGS positions (circles) to the JPL positions after removing the global rotations between the two frames. The scale of the vector module is shown in the figure. Two sources with large position differences are not shown.

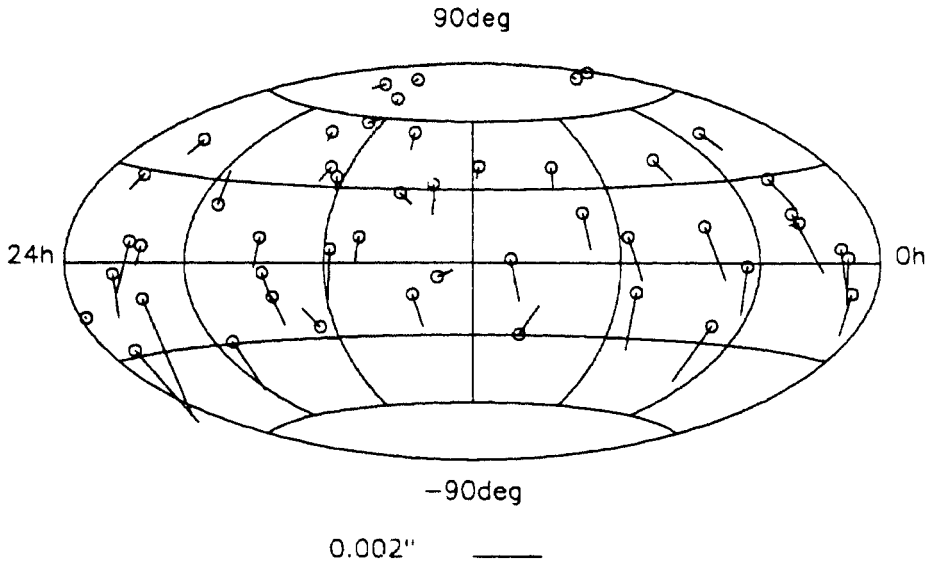

Figure 13c. Position differences of radio sources common to NGS and USNO frames in Aitoff projection. The solid lines join the NGS positions (circles) to the USNO positions after removing the global rotations between the two frames. The scale of the vector module is shown in the figure.

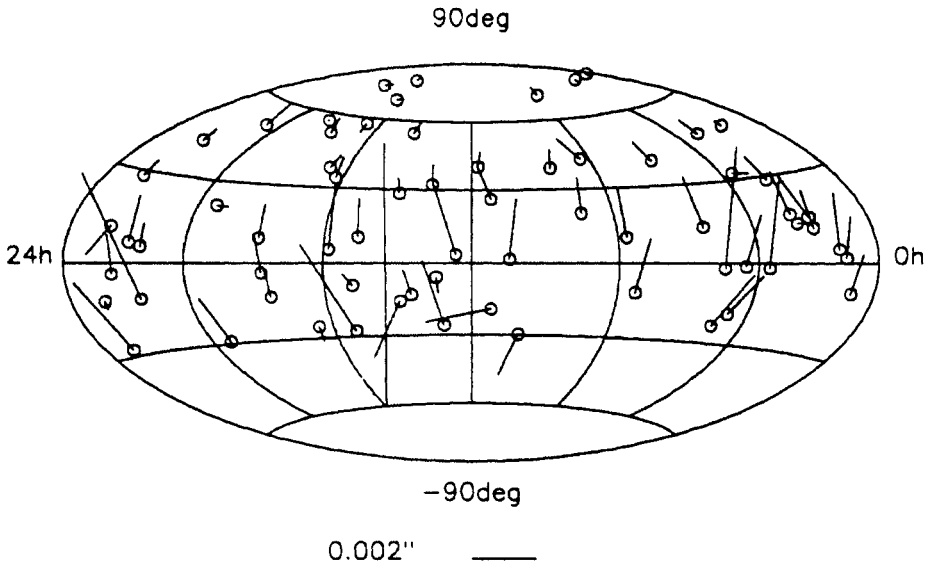

Figure 13d. Position differences of radio sources common to USNO and GSFC frames in Aitoff projection. The solid lines join the USNO positions (circles) to the GSFC positions after removing the global rotations between the two frames. The scale of the vector module is shown in the figure.

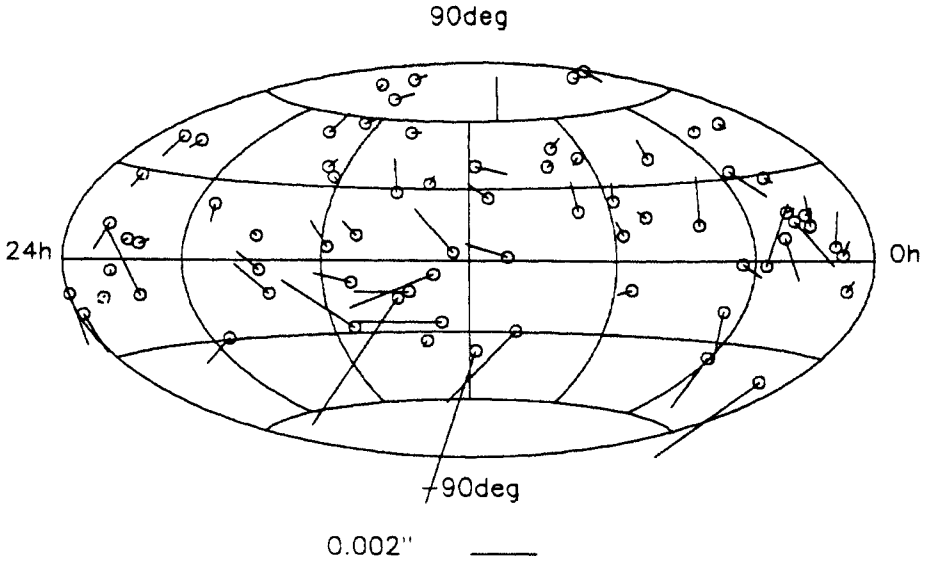

Figure 13e. Position differences of radio sources common to USNO and JPL frames in Aitoff projection. The solid lines join the USNO positions (circles) to the JPL positions after removing the global rotations between the two frames. The scale of the vector module is shown in the figure. Four sources with large position differences are not shown.

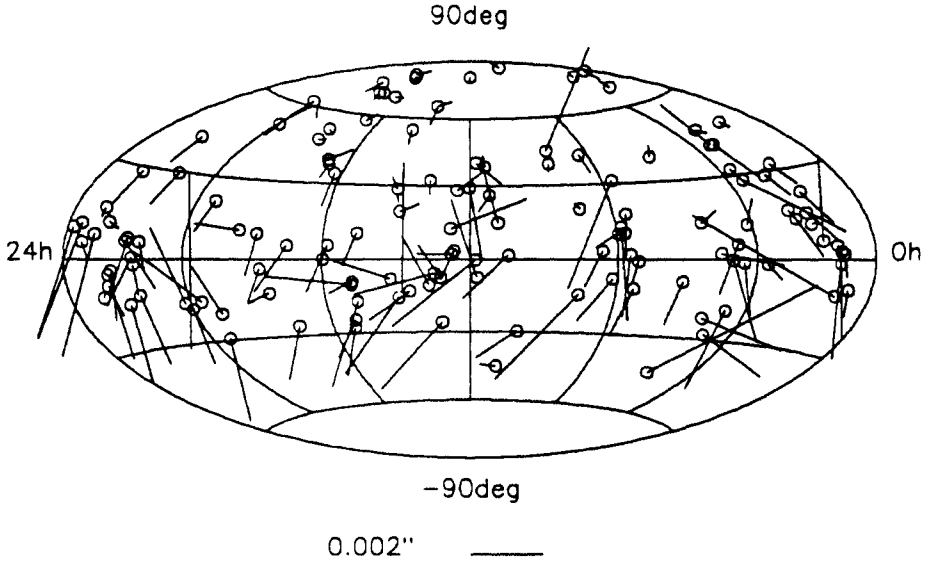

Figure 13f. Position differences of radio sources common to GSFC and JPL frames in Aitoff projection. The solid lines join the GSFC positions (circles) to the JPL positions after removing the global rotations between the two frames. The scale of the vector module is shown in the figure. Fifteen sources with large position differences are not shown.

Analysis of RSC(IERS) 91 C 01

The initial realization of the IERS Celestial Reference Frame, RSC(IERS) 88 C 01, (Arias *et al.*, 1988) included a total of 228 extragalactic radio sources. In the normal process of IERS global analyses, the ICRF is re-evaluated whenever new information is available. This is a maintainance process, in which strict rules are applied, with the aim of insuring the consistency of the direction of axes with the initial definition, while improving the accuracy of the existing sources and extending the frame to new sources.

The adjustment of the celestial reference frame is one part in an algorithm which also embodies maintenace of the terrestrial frame and of consistent series of EOP over the years. This approach makes it possible to compare the corresponding elements in the various individual solutions, thus providing an external check of the consistency of the models used. In the case of the celestial frames, the model for comparisons is a three-angle rotation. The consistency checks are based on a comparison of rotation angles between reference frames with systematic differences between time series of universal time and of the celestial pole offsets (Feissel, 1991). The practical implementation which led to RSC(IERS) 91 C 01, published in the IERS Annual Report for 1990, is described here.

RSC(IERS) 91 C 01 results from the combination of two frames obtained independently by analysis centres at Goddard Space Flight Center (GSFC) and Jet Propulsion Laboratory (JPL).The coordinates of the 334 objects in RSC(GSFC) 91 R 04 are evaluated from data acquired since 1979 by the NASA Crustal Dynamics Project (CDP), POLARIS/IRIS, the USNO NAVNET and the NRL reference frame program. The right ascension origin of the GSFC reference frame is defined by the a priori right ascension of the quasar 3C273B(1226+023). The RSC(JPL) 91 R 01 reference frame (241 objects) is elaborated from the analysis of Deep Space Network (DSN) VLBI observations. The coordinate system is tied to RSC(IERS) 89 C 01 by fixing the right ascension and the declination of 0851+202 and the declination of 0234+285 to their values in that frame. These objects are among the best observed sources in the DSN catalogue, and are primary sources in the IERS Celestial Reference Frame. Both individual reference frames are referred to J2000.0 by means of the standard IAU 1976 precession model and the IAU 1980 Theory of nutation. In their data analysis, radio source positions are obtained in parallel to an adjustment of orrections to the direction of the celestial pole given by the models. The frames have 179 objects in common.

Selection of primary sources of RSC(IERS) 91 C 01

The individual catalogues include well observed pointlike sources, with small uncertainties in their coordinates, and other sources, less observed or having sizeable structure, with coordinates of greater uncertainty. It is therefore necessary to select carefully the *primary sources* to be used in the maintenance of the frame. The 23 primary sources in the initial definition of the IERS frame were selected on the basis of structure, sky coverage, time stability and number of observations (Carter, 1987). In more recent realizations, the selection is based on statistical tests on the actual coordinates in independent programs.

Radio sources common to at least two of the frames used for the maintenance or densification, but not in the primary list, are defined as *secondary sources*, while those belonging to only one individual frame are the *complementary sources*. Neither secondary nor complementary sources are used to define the directions of axes of the combined frame; only their positions relative to it are evaluated.

The primary sources are used to maintain the direction of axes of the celestial reference frame.RSC(IERS) 91 C 01 contains 57 primary sources selected on the basis of statistical analysis performed on the VLBI catalogues described in the previous section (G91, J91, N91, U91).The method of selection of primary sources is as follows.

After solving for the rotation angles A_1, A_2, A_3 between the six pairs of frames, we performed χ^2 tests on the post-fit residuals, for right ascensions and declinations separately, and for both coordinates together. The procedure used a recurrent elimination of sources with the largest position discrepancies until a normal distribution is reached. Table 15 shows, for each pair of catalogues, the χ^2 obtained for the normal distribution, the number of times the rms of the residuals considered as a limit value, and the percentage of objects rejected.

Table 15. Results of the elimination of radio sources to obtain a normal distribution of post-fit residuals.

Frame 1-Frame 2	χ^2			rejected
	α	δ	$\alpha+\delta$	obj.(%)
NGS - GSFC	1.0	1.5	1.6	10
USNO - GSFC	1.9	0.9	1.4	2
GSFC - JPL	1.6	1.3	1.1	19
NGS - JPL	1.5	1.3	1.6	4
NGS - USNO	1.8	1.0	0.9	0
USNO - JPL	1.1	1.2	1.5	8

From the six comparisons of frames, 100 radio sources provide a normal distribution of residuals after taking out the relative orientations between frames. However, we have retained as primary sources only those objects contained at least in three catalogues, resulting in a set of 57 primary sources. These sources are distributed in the declination range $-45° < \delta < +74°$, 41 of them in the northern hemisphere and 16 in the southern hemisphere. The coordinates of the 57 sources in RSC(IERS) 91 C 01 are listed in table 16. 44 objects with post-fit residuals following a normal distribution were not included in the primary list because they belong only to two frames and they permit only one comparison. These objects can be considered good candidates to become primary in the future, provided that they will be included in more than two VLBI solutions. They are evenly distributed in both hemispheres (see table 17).

In the previous realization of the IERS celestial reference frame, RSC (IERS) 90 C 01 (IERS, 1990), the 51 sources retained as primary were those which showed position differences smaller than 0.0015" in all possible comparisons between the four 1990 catalogues of table 8, after taking out the relative orientations. Even if the criteria applied in the selection of primary sources in RSC (IERS) 90 C 01 and in RSC (IERS) 91 C 01 seem formally different, they lead almost to the same set. The residuals of only three primary sources of the previous realisation were rejected by the χ^2 test.

In parallel to the statistical analyses of the object coordinates available from various analysis centres, checks of the size and variability of the radio sources are also performed using maps available in the literature (*e.g.*, Charlot, 1990).

Table 16. Sources used to maintain the axes of RSC(IERS) 91 C 01 (primary sources)

Radio Source Coordinates RSC(IERS) 91 C 01

SOURCE	RIGHT ASCENSION	DECLINATION	UNCERTAINTY	
	h m s	° ' "	s	"
0016+731	0 19 45.786404	73 27 30.01761	0.000081	0.00024
0048-097	0 50 41.317360	- 9 29 5.20906	0.000016	0.00031
0106+013	1 8 38.771065	1 35 0.31788	0.000016	0.00027
0119+041	1 21 56.861675	4 22 24.73538	0.000016	0.00030
0133+476	1 36 58.594799	47 51 29.10023	0.000021	0.00024
0201+113	2 3 46.657040	11 34 45.41044	0.000021	0.00038
0229+131	2 31 45.894035	13 22 54.71659	0.000016	0.00024
0234+285	2 37 52.405659	28 48 8.99027	0.000017	0.00024
0235+164	2 38 38.930080	16 36 59.27506	0.000016	0.00024
0300+470	3 3 35.242210	47 16 16.27571	0.000019	0.00024
0333+321	3 36 30.107637	32 18 29.34219	0.000025	0.00030
0336-019	3 39 30.937769	- 1 46 35.80314	0.000016	0.00028
0420-014	4 23 15.800691	- 1 20 33.06483	0.000016	0.00025
0434-188	4 37 1.482683	-18 44 48.61213	0.000018	0.00030
0528+134	5 30 56.416725	13 31 55.15023	0.000016	0.00024
0552+398	5 55 30.805599	39 48 49.16540	0.000016	0.00024
0727-115	7 30 19.112469	-11 41 12.59978	0.000017	0.00028
0742+103	7 45 33.059502	10 11 12.69292	0.000016	0.00026
0814+425	8 18 15.999644	42 22 45.41503	0.000019	0.00026
0823+033	8 25 50.338356	3 9 24.52052	0.000016	0.00026
0851+202	8 54 48.874924	20 6 30.64131	0.000016	0.00025
0923+392	9 27 3.013887	39 2 20.85193	0.000016	0.00024
1055+018	10 58 29.605223	1 33 58.82409	0.000016	0.00027
1104-445	11 7 8.694184	-44 49 7.61854	0.000036	0.00033
1123+264	11 25 53.711910	26 10 19.97878	0.000016	0.00025
1144+402	11 46 58.297905	39 58 34.30477	0.000023	0.00034
1156+295	11 59 31.833895	29 14 43.82718	0.000023	0.00034
1222+037	12 24 52.421886	3 30 50.29375	0.000021	0.00048
1226+023	12 29 6.699768	2 3 8.59897	0.000023	0.00029
1308+326	13 10 28.663847	32 20 43.78289	0.000016	0.00026
1334-127	13 37 39.782803	-12 57 24.69244	0.000019	0.00032
1354+195	13 57 4.436638	19 19 7.37243	0.000016	0.00029
1404+286	14 7 0.394398	28 27 14.69019	0.000020	0.00031
1418+546	14 19 46.597378	54 23 14.78700	0.000023	0.00029
1502+106	15 4 24.979786	10 29 39.19905	0.000016	0.00031
1510-089	15 12 50.532932	- 9 5 59.82878	0.000019	0.00032
1519-273	15 22 37.675987	-27 30 10.78429	0.000022	0.00047
1548+056	15 50 35.269253	5 27 10.44862	0.000019	0.00032
1611+343	16 13 41.064232	34 12 47.90897	0.000016	0.00030
1633+382	16 35 15.492952	38 8 4.50064	0.000017	0.00030
1641+399	16 42 58.809925	39 48 36.99405	0.000016	0.00030
1730-130	17 33 2.705772	-13 4 49.54727	0.000019	0.00033
1739+522	17 40 36.977818	52 11 43.40752	0.000022	0.00033
1741-038	17 43 58.856155	- 3 50 4.61603	0.000018	0.00032
1749+096	17 51 32.818573	9 39 0.72885	0.000018	0.00032

Table 16 (Cont.)

Radio Source Coordinates RSC(IERS) 91 C 01

SOURCE	RIGHT ASCENSION	DECLINATION	UNCERTAINTY	
	h m s	° ' "	s	"
1958-179	20 0 57.090431	-17 48 57.67130	0.000020	0.00033
2113+293	21 15 29.413446	29 33 38.36711	0.000019	0.00030
2121+053	21 23 44.517361	5 35 22.09380	0.000018	0.00031
2128-123	21 31 35.261730	-12 7 4.79533	0.000018	0.00032
2145+067	21 48 5.458663	6 57 38.60467	0.000016	0.00030
2200+420	22 2 43.291355	42 16 39.98011	0.000020	0.00027
2216-038	22 18 52.037727	- 3 35 36.87867	0.000019	0.00032
2230+114	22 32 36.408894	11 43 50.90447	0.000016	0.00029
2234+282	22 36 22.470835	28 28 57.41348	0.000018	0.00028
2243-123	22 46 18.231970	-12 6 51.27670	0.000019	0.00034
2251+158	22 53 57.747936	16 8 53.56139	0.000018	0.00029
2345-167	23 48 2.608485	-16 31 12.02074	0.000021	0.00032

Table 17. Candidate primary sources selected in the analysis for RSC(IERS) 91 C 01

Object	Object	Object	Object	Object
0112-017	0637-752	1124-186	1638+398	2223-052
0149+218	0716+714	1128+385	1656+053	2227-088
0202+319	0723-008	1150+812	1657-261	2255-282
0208-512	0735+178	1313-333	1738+476	2355-106
0256+075	0736+017	1342+663	1807+698	
0309+411	0748+126	1406-076	1823+568	
0402-362	0754+100	1504-166	1831-711	
0430+052	0805-077	1514-241	1954+513	
0440-003	0919-260	1555+001	2021+614	
0605-085	0954+658	1622-253	2131-021	

The combination model

The differences between catalogues are expressed in a direct trirectangle coordinate system with the x-axis and z-axis in the respective directions to the origin of right ascensions and pole of the IERS celestial frame. The model currently used considers a three-angle rotation matrix, assuming no systematic local deformation (see p. 28, this volume); the validity of the latter assumption is a part of the examination of the results. There is two steps in the compilation of RSC(IERS) 91 C 01. In step 1 the coordinates of the primary sources in the combined frame and the relative orientations $A_1(i)$, $A_2(i)$, $A_3(i)$ between it and the three individual frames (i=1, 2) are evaluated simultaneously by a weighted least squares adjustment. The directions of axes are constrained to be aligned with the axes of the previous realisation, RSC(IERS) 90 C 01. The consistency of the directions of axes of the successive realizations of the IERS celestial reference system already performed to date is estimated by the rotation angles from one version to the next, listed in table 8. The instability between the successive versions of the frame is presently well under 0.0001". In step 2 the coordinates of secondary and complementary sources in the combined frame are obtained by removing in each individual frame the relative orientation evaluated in step 1.

Comparison of two methods of combination

Recently, Sovers (1991b) produced a celestial frame with 216 objects by combining the 320 000 observations accumulated between 1978.6 and 1990.8 in the Crustal Dynamics Project (178 24-hour sessions, 135 000 observations, 76 objects), the IRIS program (452 24-hour sessions, 168 000 observations, 31 objects), the JPL Radio Reference Frame Development program (78 mainly 24-hour sessions, 10 000 observations, 230 objects), and the Time and Earth Motion Precision Observations program (663 3-hour sessions, 7000 observations, 106 objects). The CDP and IRIS data represent a large number of observations (see pp. 10-18) of relatively few objects made on a wide variety of networks in the northern hemisphere. The JPL data represent a large number of objects, observed with the three Deep Space Network stations which include one station in the southern hemisphere, with fewer observations of each source (see pp. 10-18), on longer baselines and with larger antennas than for CDP and IRIS. This reference frame, JPL 1990-3, is referred to as RSC(JPL) 90 R 03 in the following.

In comparison, RSC(IERS) 91 C 01 contains 396 objects. It was produced from the combination of two frames, obtained by GSFC (Ma and Caprette, 1991) and JPL (Steppe *et al.*, 1991) from two independent sets of observations which largely overlap the above ones. The JPL frame, RSC(JPL) 91 R 01, is based on essentially the above mentioned JPL observations; it contains 241 objects. The GSFC frame, RSC(GSFC) 91 R 04, is based on the CDP and IRIS observations above mentioned, completed up to the end of 1990, plus about 260 000 observations from 533 other sessions from the POLARIS, CDP-IRIS, NAVNET, and NRL astrometry programs. These additional observations concern only partially the sources in RSC(JPL) 90 R 03, they mainly bring new sources in the GSFC frame, which contains 334 objects.

The 216 JPL 1990-3 objects are all present in RSC(IERS) 91 C 01. 153 of them also have coordinates in the JPL and GSFC frames on which the IERS one is based. This offers the opportunity to investigate any significant difference between the two combined frames which may arise from the difference in methods of combination. Indeed it is expected that, as in the present IERS/CB algorithm the full covariance information of the individual frames that are combined is not used, local systematisms due to insufficient networks are not compensated for. The direct combination of observations is thought to be more efficient in this respect. However, as long as the networks do not cover properly the Earth, the local systematims cannot be expected to totally disappear. On the other hand, the comparison of partial frames on which the IERS/CB algorithm is based should be a more efficient tool to evaluate the accuracy of estimated coordinates than the direct combination of networks. It should be noted that for sources with structure size at the mas scale, the differences in resolution of baselines of different lengths can introduce shifts between the effective radiation centres that are observed. As in the frames presently available the source structure effects are not accounted for, inconsistencies can be expected for some sources, in the direct combination method as well as in the indirect one.

The uncertainties on the source coordinates in the two combined frames are derived from the variance information available as an output of the least square fit; they depend on the input covariance matrix of the observables and on the consistency of the data combined. In both cases considered here, the input covariance matrix is diagonal. In the case of the JPL combination, the observables are the delays and delay rates, and session-specific variance is added to account for mismodelling of some observational effects. The number of estimated parameters is about 58 000, including the 432 source coordinates. In the case of the IERS/CB combination, the observables are the differences in source coordinates in the two individual frames, and the only unknowns considered in addition to the 114 source coordinates are the angles which rotate the individual frames to the combined one. The input variance is obtained by adding quadratically the formal uncertainties provided in the individual frames (with a lower value of 0.25 mas for each). The formal uncertainty of the estimated coordinates reflect the consistency of the coordinates in the individual frames that are combined, taking into account the global relative orientations. Figure 14 shows the relationship between the formal uncertainties of the

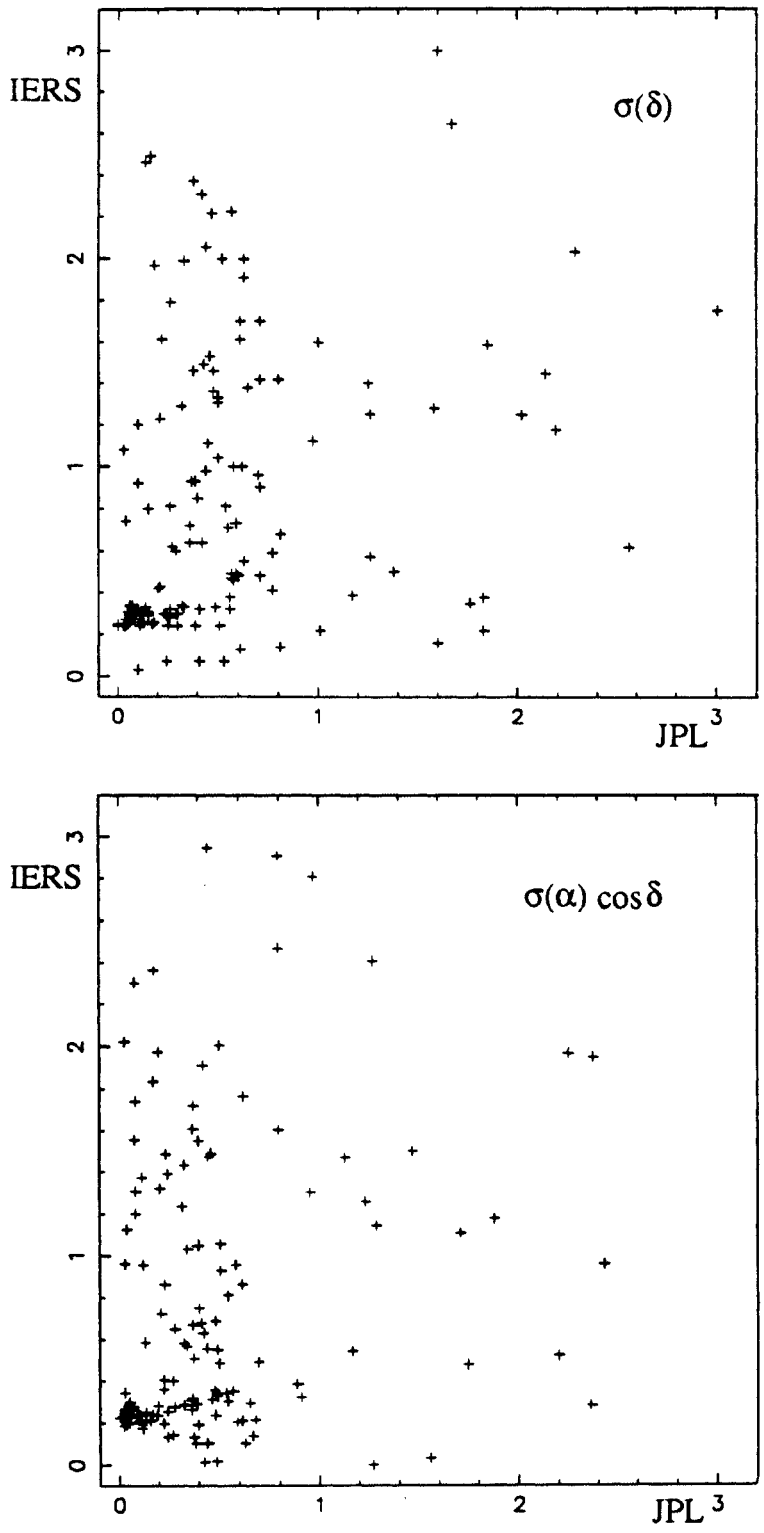

Figure 14. Formal uncertainty of the coordinates of objects in the IERS combined frame versus their value in the JPL combined frame.
Unit: 0.001".

coordinates of the same source in the two combined frames. Apart from a cluster of very small values (around 0.3 mas), the uncertainties in the IERS frame tend to be larger than in the JPL one. They are mostly smaller than 2 mas, while most of the JPL ones are smaller than 1 mas.

The differences in coordinates are investigated after taking out a global rotation between frames on the basis of the 57 primary sources of IERS (1991). The rms weighted residual in the estimation of the rotation is 0.43 mas in $\alpha \cos\delta$, and 0.61 mas in δ; the mean residual in α is negligible (0.01 mas), while it is not in δ (0.10 mas). Figure 15 shows the histogram of the residual differences between the JPL and IERS coordinates. 82% of the differences in right ascension ($\alpha \cos\delta$) are smaller than 1 mas in absolute value, but only 55% declination differences are in this range. The detailed inspection of the residuals will help characterize more precisely the declination discrepancies.

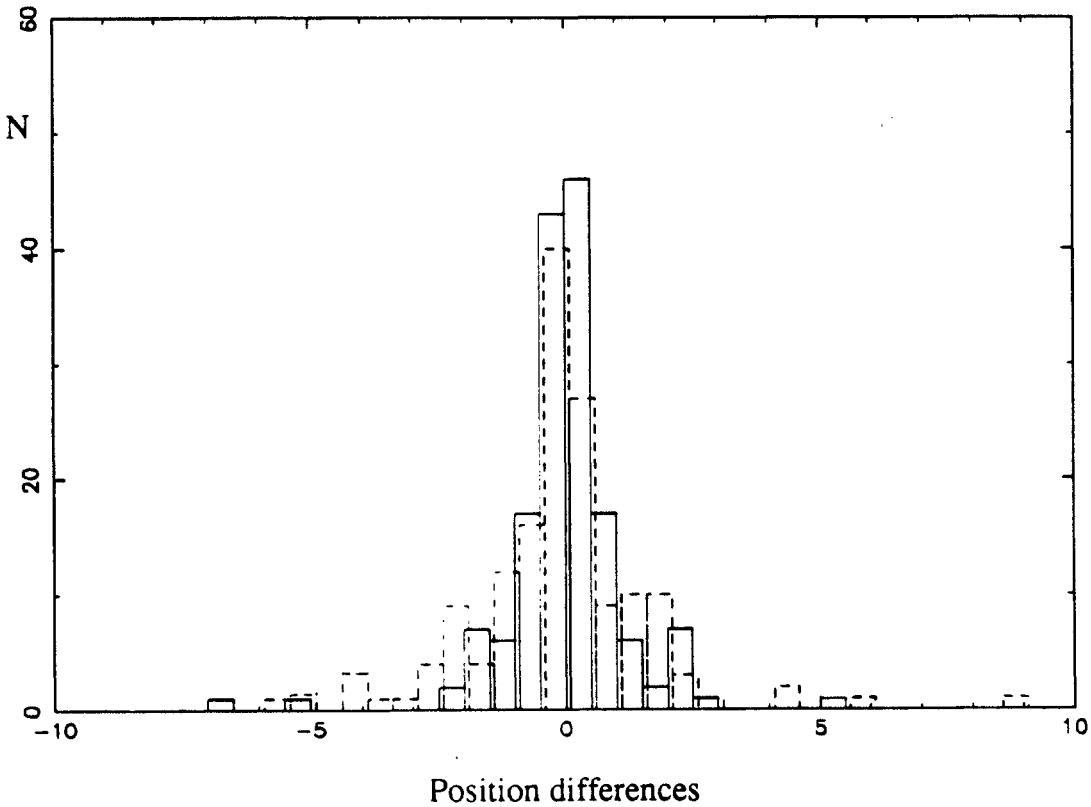

Figure 15. Histogram of position differences between the JPL and IERS combined frames (total of 151 objects). $d\alpha \cos\delta$ (solid line), $d\delta$ (dashed line). Unit: 0.001".

The residual position differences are plotted on figure 16 as a function of declination. Five of the IERS primary sources have residuals larger than 1 mas in declination, one in right ascension. The data available on them is summarized in table 18. The discrepancy in both right ascension and declination for 0016+731 seems to be due to an insufficient number of observations on the JPL side. The declination discrepancies for 0434-188, 1519-273 and 1958-179 correspond to a disagreement between the GSFC and JPL individual solutions, and the one for 1104-445 to a disagreement of the JPL combined solution with both individual solutions.

The inspection of the plot rather suggests the existence of a step of about 0.5 mas amplitude south of -5° for the declinations. Note a cluster of right ascension residuals around $\delta = -10°$ that are shifted by about -1 mas relative to the rest of the plot. The particular network geometries which contributed observations in each of the two analyses might explain this discrepancy. Other models can tentatively describe the discrepancies, using a weighting based on the root-sum-square of the formal uncertainties in the two combined frames, with a lowest value of 0.5 mas. This weighting does not account for a possible correlation between source coordinates in the two frames; it results in discarding the sources which have a large uncertainty in at least one of the frames. The dotted lines are weighted Vondrak (1977) smoothings of the plotted residuals. The smoothed trend in $d\alpha \cos\delta$ does not suggest any systematism in the low declinations; the linear trend estimated with the same weighting is $+5 \pm 2$ μas/degree (0.6 mas over the declination span covered by the common sources). The smoothed trend in declination shows a change for declinations lower than -5°, the estimated linear trend is $+6 \pm 3$ μas/degree (0.8 mas over the total declination span).

Figure 17 shows the same right ascension residuals as figure 16, with the formal uncertainties as given in the two combined frames. 98% of the differences are consistent with 0 in the 2.5 sigma limit when considering the IERS uncertainties, 86% for the JPL ones. The sections south of -20° and north of +50° are characterized by a larger dispersion. The IERS error bars are larger in these sections, reflecting the disagreement of the GSFC and JPL individual frames on which it is based. The error bars are not enlarged in the same manner in the JPL combined frame. The few outliers are associated with numbers of observations lower than 100 in the JPL and the GSFC individual frames.

Figure 18 gives the equivalent plots for the residual differences in declination. Here 73% of values are consistent with 0 in the 2.5 sigma limit in the IERS case, 57% in the JPL case. The above comment on the scale of JPL and IERS uncertainties in the north and south extreme sections is also valid for declinations. All differences larger 3 mas in absolute value are associated with small numbers of observations; they tend to cluster under $\delta = -14°$ and over $\delta = 50$. The only one exception is 1034-293 (marqued with an arrow) which has about 2200 observations. This source is one for which the four 1990 frames compared in the first part of this section give coordinates that are inconsistent at the 1-2 mas level (see table 10, p. 31).

It should be noted that the comparisons made here give information on the consistency and the precision of source coordinates, but not on their accuracy. Further studies should make use of the session per session covariance information and of the astrometric correction for source structure.

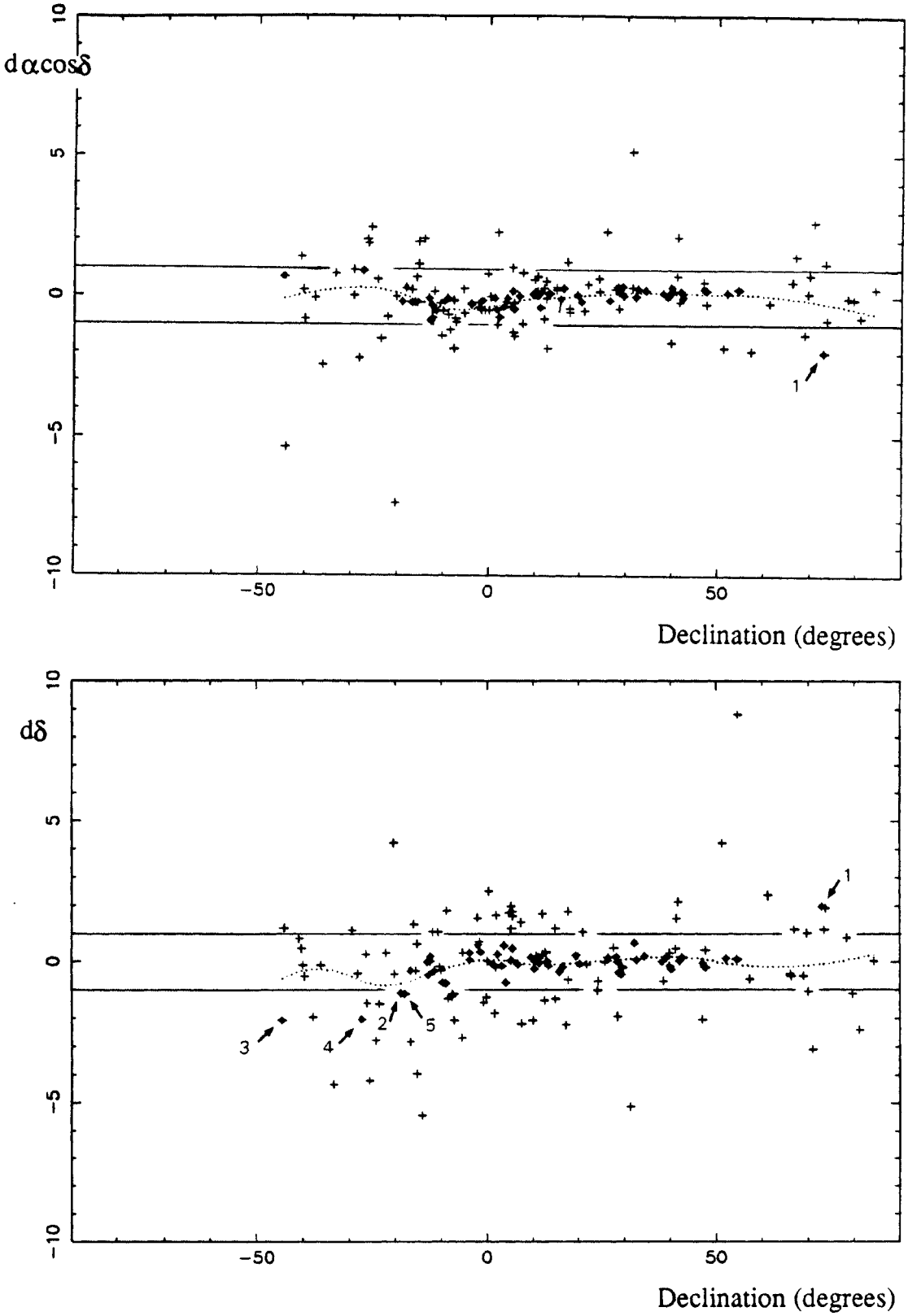

Figure 16. Residual differences in position of objects in the JPL combined frame with the IERS combined frame (JPL-IERS). The diamonds represent the IERS (1991) primary sources. The dotted line is a Vondrak smoothing of the raw differences. Unit: 0.001".

Table 18. Five IERS(1991) primary sources having large position discrepancies with JPL 1990-3

	0016+731	0434-188	1104-445	1519-273	1958-179
Number in figure 16	1	2	3	4	5
Number of observations					
JPL 1990-3	33	100	132	180	119
IERS 1991					
JPL	11	108	141	189	129
GSFC	1583	150	123	61	270
Formal uncertainty (mas)					
$\alpha \cos\delta$					
JPL comb	0.57				
IERS comb	0.24				
JPL ind	0.22				
GSFC ind	0.27				
δ					
JPL comb	0.39	0.29	0.49	0.57	0.33
IERS comb	0.24	0.30	0.33	0.47	0.33
JPL ind	0.16	0.45	0.74	0.87	0.74
GSFC ind	0.12	0.23	0.23	0.37	0.17
Residual differences (mas)					
$\alpha \cos\delta$					
JPL comb.-IERS comb	-1.98				
JPL comb.-JPL ind	-1.91				
JPL comb.-GSFC ind	-1.87				
IERS comb.-JPL ind	+0.08				
IERS comb.-GSFC ind	+0.11				
δ					
JPL comb.-IERS comb	+1.99	-1.14	-2.10	-2.06	-1.17
JPL comb.-JPL ind	+2.08	+0.12	-1.98	-1.18	-0.49
JPL comb.-GSFC ind	+1.79	-1.52	-1.96	-2.24	-1.37
IERS comb.-JPL ind	+0.09	+1.25	+0.12	+0.90	+0.69
IERS comb.-GSFC ind	-0.19	-0.36	+0.14	-0.18	-0.20

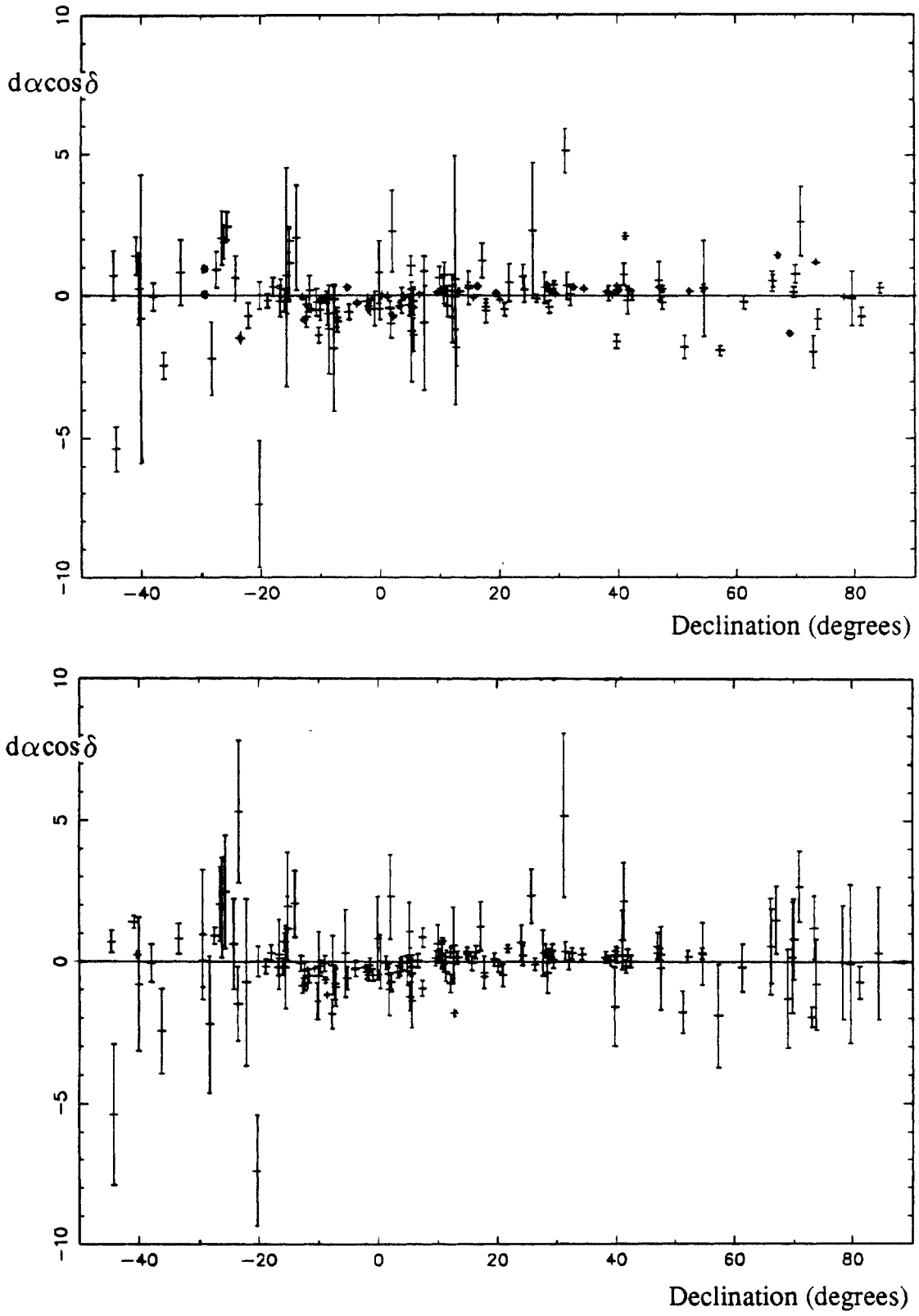

Figure 17. Residual differences in right ascension: JPL-IERS.
Upper part: with JPL error bars. Lower part: with IERS error bars.
Unit: 0.001".

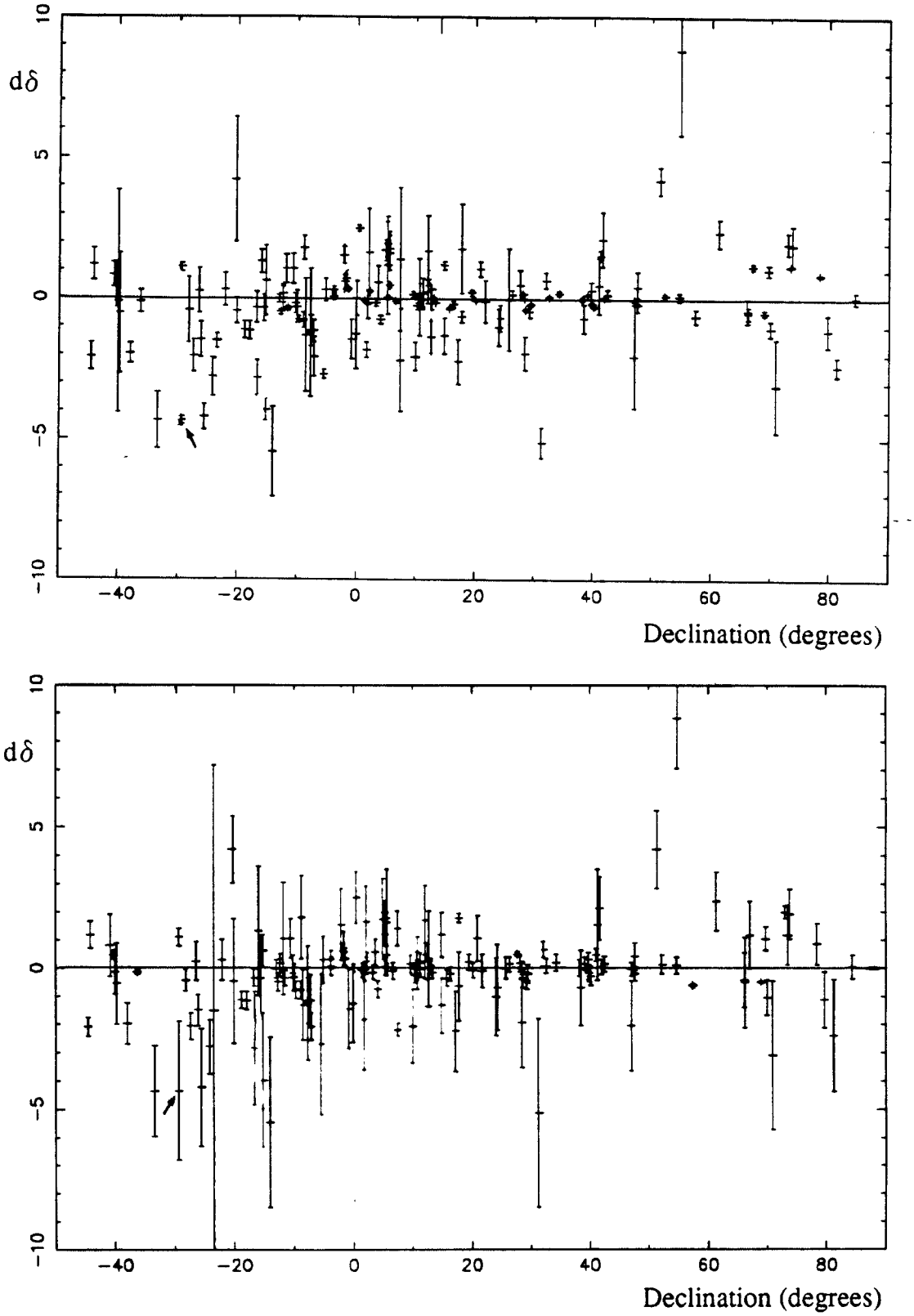

Figure 18. Residual differences in declination: JPL-IERS.
Upper part: with JPL error bars. Lower part: with IERS error bars.
Unit: 0.001".